DEFLUORIDATION OF POTABLE WATER IN CKDu PREVALENT AREAS ENRICHED WITH HARDNESS USING MODIFIED-FLY ASH FUNCTIONALIZED WITH IRON OXIDE

Edirisooriya Arachchige Chandrika Priyadarshani

(168884F)

Thesis submitted in partial fulfillment of the requirements for the degree of Master of Environmental Management

Department of Civil Engineering

University of Moratuwa

Sri Lanka

September 2020

DECLARATION

"I declare that this is my own work and this thesis does not incorporate without acknowledgement any material previously submitted for a Degree or Diploma in any other University or institute of higher learning and to the best of my knowledge and belief it does not contain any material previously published or written by another person except where the acknowledgement is made in the text.

Also, I hereby grant to University of Moratuwa the non-exclusive right to reproduce and distribute my thesis, in whole or in part in print, electronic or other medium. I retain the right to use this content in whole or part in future works (such as articles or books)."

Signature: Date:

The above candidate has carried out research for the Masters thesis under my supervision.

Name of the supervisor: Prof. M. W. Jayaweera

Signature of the supervisor: Date:

The above candidate has carried out research for the Masters thesis under my supervision.

Name of the co-supervisor: Dr. (Ms.) W. B. Gunawardana

Signature of the supervisor: Date:

Abstract

Chronic Kidney Disease of Unknown Etiology is a major health issue reported in countries around the equator including Sri Lanka, Tunisia, Andra Pradesh India, and El Salvador. In Sri Lanka, CKDu is prevalent in the North-Central Province and now it is being progressed in the dry zone. The exact causal factor for the disease is not known yet where scientists now mainly suspect that the multiple ion interaction in potable groundwater may be the root cause for the disease. Further, fluoride ion concentration is higher in CKDu prevalent areas and the interaction of fluoride ion with other constituents (Cd, As, Al, hardness) is mainly suspected as the cause for the disease. The synergistic effect of hardness and fluoride on the CKDu had been discussed in many studies worldwide where the prevalence of other ions is very less, and it is below the WHO maximum allowed concentrations. The hardness and fluoride distribution are relatively higher in CKDu prevalent areas in Sri Lanka and the nephrotoxicity of hardness and fluoride in their mutual presence is proven by experiments with mice. Our preliminary studies found that there is no CKDu when the hardness and fluoride concentrations of water are below 200.00 mg/L and 0.47 mg/L, respectively. Therefore, this study was carried out to remove the hardness and fluoride concentrations of water to the level of 200.00mg/L and 0.47mg/L, respectively. Initially, a divalent cation exchange column was designed using a commercially available cation exchange resin, ECO A, to remove excessive hardness level up to 200.00mg/L. The eluent from the cation exchange column was further treated for defluoridation. Coal derived fly ash was further modified using the hydrothermal method. The Modified Fly Ash (MFA) was further treated with Fe (III) Chloride to generate positive charges on the surface. FTIR, SEM, EDX, confirmed the incorporation of Fe into MFA and, the defluoridation ability of Fe functionalized MFA. FTIR spectra ($400cm^{-1}$ – $600cm^{-1}$ region) showed the incorporation of Fe into MFA. The average crystalline size obtained from XRD analysis was 23.3nm and the synthesized material was in nanoscale. The batch experiments showed that 1.3g of the Fe functionalized MFA resulted in the maximum defluoridation for a 100.00 ml of water sample containing 200.00 mg/L hardness and 2.00 mg/L fluoride within 40 minutes of contact time at pH 6. The material gave optimum defluoridation at pH 6 and therefore there is no need of altering the pH of water for the defluoridation. The adsorption data fitted with the Langmuir adsorption isotherm where the maximum adsorption capacity was 10.00mg/g. The separation factor for the Langmuir adsorption was 1.23 and therefore the Langmuir adsorption is favorable. The reaction followed pseudo second order kinetics. Regeneration studies of the Fe functionalized MFA showed that

NaOH was the best regeneration agent and the material was exhausted after two regeneration cycles. The material synthesize cost to purify water for a five-member family for three months was LKR 6923.07 (37.52USD) and the cost for the regeneration was LKR 174.46 (0.95USD). Therefore, the synthesized material is ideal and cost effective to remove fluoride in potable ground water in CKDu prevalent areas.

.

Key Words: CKDu, Functionalized Modified Fly Ash (FMFA), Defluoridation, Fluoride, Hardness, Adsorption, Iron Oxide

ACKNOWLEDGEMENT

First and foremost, I would like to extend my heartfelt gratitude to my supervisor Prof. Mahesh. Jayaweera, for providing me the opportunity to complete the research. Your guidance and encouragement given at every step of the way in the research helped me to achieve the goals. Your support was immense, and I am very fortunate to have you as my supervisor. I extremely appreciate the advice given in experiments, writings, and moral assistance given to complete this research.

I am very grateful to my co-supervisor Dr. Buddhika Gunawardana, for providing her guidance and support for the research project. Your feedback on my experiments, writing, helped me to complete a very productive study. Furthermore, I would like to extend my gratitude to Prof. Jagath Manatunge for guiding me to conduct a fruitful and successful research. Your advice and guidance helped me to think out of the box.

I wish to express my sincere thanks to the laboratory staff of Environmental Engineering Laboratory, Department of Civil of Engineering, University of Moratuwa; Ms. Nilanthi Gunathilake Mr. Kasun Zoysa, Mr. Justin and Mr.Dhananjaya and Ms. Nipuni for the assistance received to conduct my research experiments successfully in the Environmental engineering laboratory.

I would like to thank the head and the staff of Analytical Laboratory, Department of Materials Science and Engineering, University of Moratuwa for allowing me to use laboratory equipment.

I would like to thank Madhurangi, Madhusha and Gimhani and Thilini for their friendship, guidance, strength, and assistance given in the period of the research study.

I am grateful to my family for being there for me, giving their unconditional love and support to fulfill my aims. Finally, I would like to thank my spouse and baby for supporting, encouraging, and understanding me in my quest.

TABLE OF CONTENTS

TABLE OF FIGURES

LIST OF TABLES

LIST OF ABBREVIATIONS

Abbreviation	Description
CKD	Chronic Kidney Disease
CKDu	Chronic Kidney Disease of unknown etiology
CFA	Coal Fly Ash
MFA	Modified Fly Ash
FMFA	Iron oxide Functionalized modified Fly Ash
(FMFA) opt	Optimized Iron oxide Functionalized modified Fly Ash
IC	Ion Chromatography
GFR	Glomerular filtration rate
SL	Sri Lanka
NCP	North Central Province
FTIR	Fourier-transform infrared spectroscopy
SEM	Scanning electron microscope
EDX	Energy-dispersive X-ray spectroscopy
XRD	X-ray Diffraction Analysis

1 INTRODUCTION

1.1 General

Chronic kidney disease (CKD) is a major problem in the health care system of Sri Lanka. Diabetes and various forms of glomerulonephritis are well-recognized etiologies (Rodrigo et al., 2013). Three decades ago, a new type CKD, where no exact cause is confirmed, is being progressed in Sri Lanka. This new CKD caused a rise in the prevalence of CKD in the country and it had been recognized as chronic kidney disease of unknown etiology (CKDu) (Gooneratne et al., 2008). Equal scenarios with no exact cause for CKD have been reported in some other regions in the world such as in El-Salvadore, Tunisia, India (Gifford et al., 2017). Mainly, environment-related factors and conditions, including low water quality, heavy metals, and chemicals used for industry, have been correlated to the progression of CKDu in other parts of the world (Department of Agriculture SL 2006 &Virginia et al., 2015).

Sri Lanka the population is closed to 20 million and farming plays a vital role in the economy (Department of Agriculture SL 2006). Large populations in tropical, dry regions, especially those who relate to agriculture and farming are at a huge risk of the disease (Jayatilake et al., 2013). The geographic distribution of the disease shows that only some regions in the dry zone have been affected where the disease is not prevalent in the wet zone. A changing of hydrogeochemistry might have brought about the CKDu within the last two decades (Chandrajith & Disaanayake, 2017). Most of the affected populations drink groundwater as the drinking water source (Jayatilake et al., 2013).

Contaminants in drinking water are suspected to be one of the major causative factors for CKDu (Balasooriya et al., 2019). Geographical distribution and research findings focus a multifactorial etiology, while massive attention has been drawn on the hydrogeochemistry of water (Wanigasuriya et al., 2014 & Dharma-wardana, 2014). Also, the synergistic effects of different contaminants present in potable water have been suggested as a key triggering factor for CKDu (Wimalawansa, 2015).

Furthermore, Fluoride in water, individually or combined with other co-contaminants including heavy metals (As and Cd) and hardness are being suspected as a major cause for the CKDu (Dharma-wardana, 2014). Based on the geographical distribution of fluoride levels in groundwater and the CKDu prevalence in Sri Lanka, it shows a positive correlation where increased fluoride levels in water correlate to a higher number of CKDu patients (Chandrajith and Dissanayake, 2017). According to the Hydro-geochemical Atlas of Sri Lanka published by Dissanayake and Weerasooriya (1985), it is observed that high concentrations of groundwater fluoride vary from 0.05 to 4.8 mg/L, with the mean value of 0.78 mg/L, which is far above the 0.5 mg/L, the limit recommended by WHO for tropical countries (Wimalawasha et al., 2014 and Chandrajith et al., 2011). Chandrajith and co-workers have studied the disease progressing pattern of the CKDu and found that the disease is prevalent in the fluoride-rich regions (Chandrajith et al., 2012). This evidenced that groundwater fluoride and its interactions with other ions in water including hardness, Cd, and Al plays an important role in the prevalence of CKDu. Moreover, studies from several other countries provide evidence of a relationship with groundwater as one of the major risk factors for kidney diseases (Bober et al., 2006; Chouhan and Flora, 2008).

The major components that interact with fluoride to enhance its nephrotoxicity include hardness, Cd, and Al (Dharma-wardana, 2017, Wasana et al., 2015). Moreover, according to the experiments done by Wasana et al. (2015), no nephrotoxicity has been observed when fluoride ions alone are present in water as high as 18 mg/L which is 12 times higher than the maximum allowed level by WHO (1.5 mg/L). In addition to fluoride, the Calcium and Magnesium hardness in potable waters of CKDu prevalent areas have reported high values ranging from 100 — 600 mg/L (Chandrajith et al., 2011). The number of CKDu patients is higher in the areas where the hardness and fluoride in water is comparatively high. On the other hand, the levels of Cadmium present in drinking water in NCP is below WHO recommended maximum tolerance limit of 5 μg/L (WHO 2012; Wasana et al. 2012; Jayatilake et al., 2013). No nephrotoxic effect due to the formation of Al-F complexes has been discussed in

Dharma-wardane (2017). Thus, based on the experiments done by Wasana et al., 2015, review on the effect of multiple ion interactions on CKDu by Dharma-wardene (2017), and the geographical distribution of hardness, fluoride, and the number of CKDu patients in CKDu prevalent areas, it is obvious to suggest the relationship between hardness, fluoride, and its combined effect on nephrotoxicity.

Therefore, this study focuses on investigating the effect of hardness and Fluoride on CKDu and removal of either of a compound to a desirable limit to overcome the synergistic toxicity caused in their mutual presence to a safe level by the development of an ion-exchange column for excessive hardness removal and, synthesis of a material for effective defluoridation in the presence of hardness.

Modified fly ash (MFA) derived from coal fly ash was impregnated with iron oxide to study the potential of modified fly ash functionalized with iron oxide (FMFA) for an effective defluoridation in the presence of hardness. The FMFA material was synthesized using different ratios of MFA: Fe and the optimized weight combination of MFA: Fe was selected based on the highest Fluoride removal. The optimum FMFA dose was obtained to eliminate the synergic effect of fluoride and hardness by reducing the fluoride level to 0.5 mg/L or below, assuring the incoming permeate water has no nephrotoxic effect from hardness and fluoride in their mutual presence.

1.2 Objectives

The overall objective of this study is to defluoridation of potable water enriched with hardness using modified fly ash functionalized with iron oxide.

Specific objectives

1. Establishment of the distribution of fluoride and hardness levels of potable water for different geographical locations in CKDu prevalent areas, and CKDu non-prevalent areas and studying the linkage between the different hardness levels and different fluoride levels on CKDu prevalence.

2. Development of an ion-exchange column to remove excessive hardness to a desirable level.

3. Development of a suitable material for effective defluoridation in CKDu prevalent areas in the presence of hardness.

1.3 Approach

Chapter 1 is the introduction to the research study basically on the prevalence of CKDu in Sri Lanka and the world, the plausible causal factors for CKDu, the possible nephrotoxic effects between hardness and fluoride in potable water in their mutual presence in CKDu prevalent areas, the need of discontinuing this synergy by the removal of each ion to a safe level applying selecting a most suitable method and the overall objective and the specific objectives of this study.

Chapter 2 discusses the literature available on the global and local distribution of CKDu, the plausible causal factors identified, the effect of multiple ions present in potable water on CKDu, the nephrotoxicity caused by hardness and fluoride in their mutual presence, and possible available defluoridation techniques.

Chapter 3 describes the materials and methods used in this research project. Procedures followed to achieve each objective, experimental setups, and methodologies applied for the generation of adsorbent and defluoridation and regeneration and isotherm and kinetic studies on defluoridation.

Chapter 4 presents the results and discussion for every experiment done during the research project. The distribution of fluoride and hardness of potable water for different geographical locations in CKDu prevalent areas and non-prevalent areas was established and the linkage between the mutual presence of fluoride and hardness and CKDu prevalence was studied. Methods applied for an effective removal of hardness and fluoride are interpreted. Moreover, the results and discussions on the batch studies to select optimum conditions and dosages of adsorbents, the kinetic and isotherm studies

on defluoridation with the aid of synthesized material, and finally the regeneration of the synthesized material is discussed.

Chapter 5 contains the conclusion and recommendations of the study.

2 LITERATURE REVIEW

2.1 What is CKDu?

Sri Lanka recently transformed from a low- to middle-income country, and its disease pattern has been moved from infectious and maternal/childhood diseases towards non-communicable diseases (NCDs) (Ministry of Health Sri Lanka, 2018). The progression and associated lethality of chronic kidney disease (CKD) are being risen in Sri Lanka over the last two decades with a trend of being magnified since the last decade due to the emergence of a new form of CKD of unknown etiology (CKDu). Particularly, CKDu is unknown and it is not associated with either hypertension, diabetes, or other aetiologies typically associated with traditional CKD. This arising disease is increasing slowly, non-reversible, and asymptomatic till ultimate stages with histopathological features are identified by renal biopsies indicating tubulointerstitial fibrosis and tubular atrophy (Athuraliya et al., 2011).

2.2 Global Distribution of CKDu

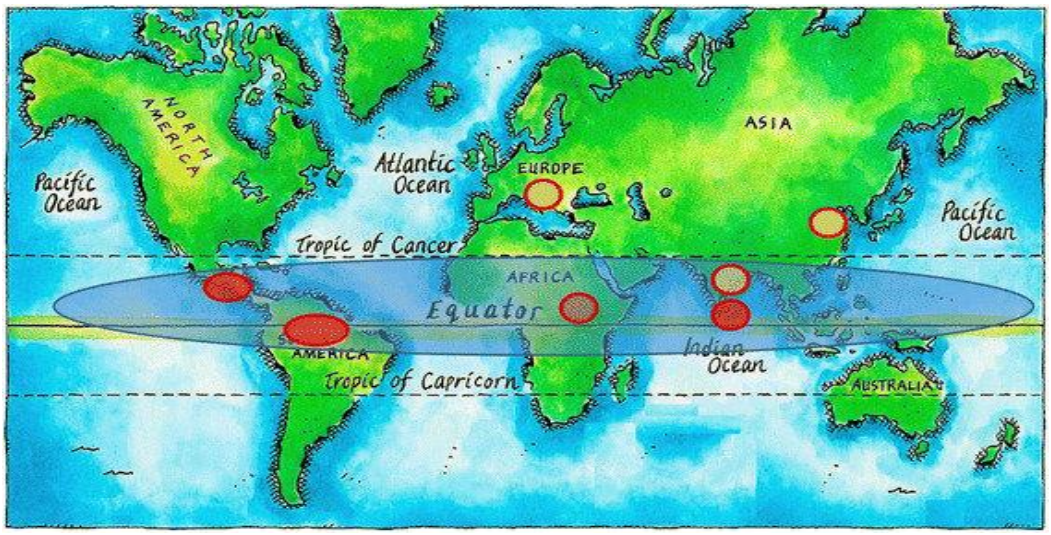

Figure 2.1 The Global distribution of CKDu (Wijewansha et al., 2018)

Chronic kidney disease of unknown etiology was firstly up started to appear in the early 1960s in the Balkan regions (Grollman et al., 2006) and after it had appeared among the countries near the equator including Central America (Koh et al., 1996).

In addition to a fatal disease, CKDu has become a critical socio-economic and environmental crisis. The disease is being rapidly manifested in countries near the equator and found in agricultural societies of economically poor regions close to the equator (Correa-Rotter et al., 2014; Roncal-Jimenez et al., 2016). North Central Province of Sri Lanka (NCP) has also been subjected to extensive research at the local level (Giffored et al., 2017).

2.3 CKDu in Sri Lanka

An increasing number of Sri Lankans suffer from CKDu since the 1990s; more than 50,000 patients have been diagnosed with late-stage kidney disease. From the CKD patients in Sri Lanka, 10% of the adult population is affected by this disease (Ileperuma 2012). The death ratio of the disease is 3% and the doubling time of no of CKDu patients has been reported as 4-5 years (Wimalawansa., 2015). Many of these patients are reported from the North Central (NCP) and North Western (NWP) Provinces of Sri Lanka and considerable amounts of patients have been reported from Uva, Eastern, and Northern Provinces (Chandrajith et al., 2011). Medawachchiya, Padaviya, Siripura, Horowpathana, Medirigiriya, Polonnaruwa, Nikawewa, Dehiattakandiya, Girandurukotte, Nikawewa, and Wilgamuwa are some of the recognized CKDu prevalent regions (Jayasekara et al., 2013 and Chandrajith et al., 2011) where, rural male paddy farming community has become the most affected category from the reported CKDu patients (Athuraliya et al., 2011).

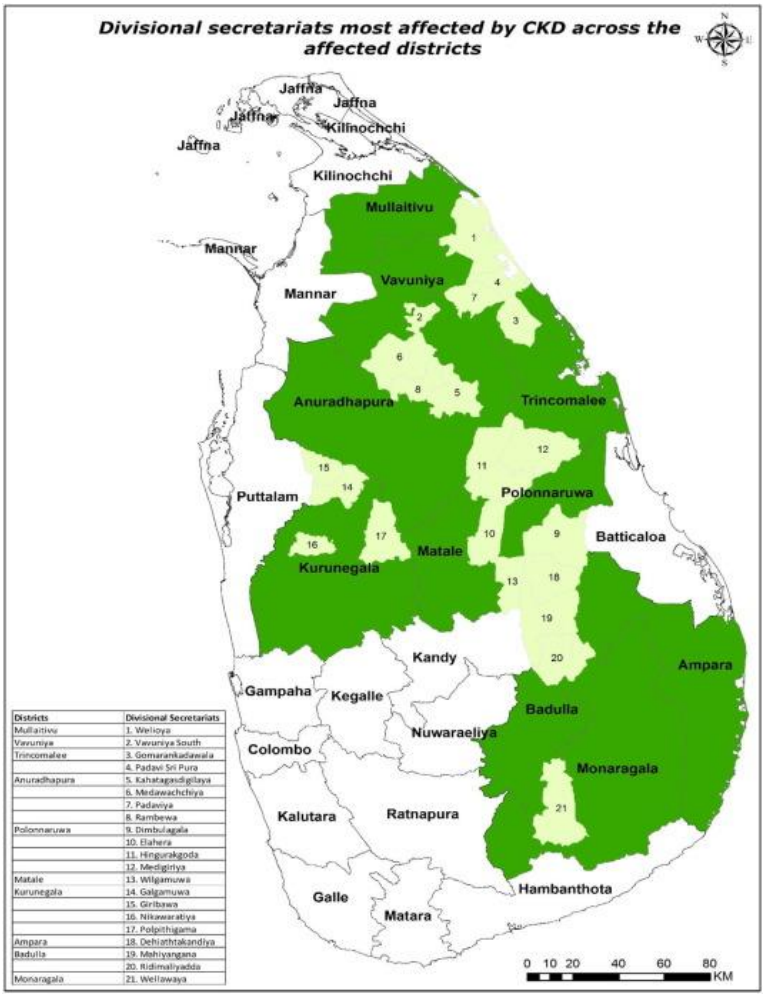

Figure 2.2 Divisional Secretariats most affected by CKD (Cafle et al., 2019)

The reported CKDu patients are between 17–70 years of age, and most of them are men. Most of the affected men are between 30-60 years and in their productive working age (Chandrajith et al., 2011), and therefore the disease causes a huge social and economic burden at the individual and national level (Weerasooriya et al., 2019).

2.4 The Prevailing Climatic conditions in the North Central Province

The NCP is the largest province in Sri Lanka, covering 5.5% of the total population in Sri Lanka. It is in the dry zone of Sri Lanka and the mean annual rainfall is about 1250

mm and the average daytime temperature is between 25–30 °C (Department of Meteorology of Sri Lanka, 2012).

The NCP gets rain from is from October to January which brings around 80% of the annual rainfall. From May to September is the prolonged dry period with vigorous desiccating winds. There is about 1700 and 1900 mm of mean evaporation rate is reported in the region, implying water stress during the dry period of the year. Large-scale industrial activities are nonexistent in NCP. Agriculture is the main sector of employment with more than 50% of the population involved in farming (Central Bank of Sri Lanka, 2010). NCP has a cascade irrigation system where the agricultural fields are fed by irrigation canals from reservoirs. The reservoirs are fed by river diversions from the middle of the country which is free from CKDu. In a cascade irrigation system, agrochemical washout tends to accumulate downstream (Gunatilake and Illangasekera, 2015; Jayasumana et al. 2017). However, the affected community does not obtain drinking water from irrigation canals or reservoirs. Pipe-borne drinking water is available to only 16% of the total population (Perera et al., 2008). The rest of the drinking water requirements of NCP are met by spring wells and shallow wells. Springwater is less likely to contaminate from irrigation canals as they originate from the deeper quartzite formation, but shallow wells are more contaminated by irrigation water (Jayasumana et al., 2017). A low prevalence of CKDu has been reported among consumers of spring water (1.5%), and high prevalence (7.7%) among consumers from shallow wells in the endemic area of Sri Lanka (Jayasekara et al., 2015)

2.5 Plausible Causal Factors for CKDu

It is hypothesized from the distribution and epidemiology that the condition is linked to the environment and is likely to be related to human activities, agriculture.

Despite available data suggesting that CKDu is an environmentally acquired disease, no definitive causative factor has been identified. Geographic distribution and research findings favor a multifactorial etiology (Rajapakse et al., 2016).

Effect of Agricultural Practices on CKDu

When in agricultural practices, the role of pesticide and heavy metals in water as a causal factor for CKDu plays a major role. Among the agrochemicals, Glyphosate is a widely used herbicide in the CKDu endemic area of NCP in paddy farming. Glyphosate has strong metal-chelating properties which are found to cause CKD by complexation with the hardness of water by forming nephrotoxic metallic compounds (Jayasumana et al. 2014). These authors explain glyphosate–metal complexation to play a major role in the CKDu. However, according to Dharma-wardana (2018), glyphosate–metal complexation cannot explain toxicity, as these complexes are insoluble forming precipitates in water. Moreover, according to the experiments done by Shankani et al. (2018), trace levels of glyphosate (1–4 mg/L) were detected in groundwaters of CKDu prevalent areas where USEPA has set the Maximum Contaminant Level (MCL) for glyphosate as 700 mg/L, i.e., the concentration below which human health effects are not expected to occur (U.S. Environmental Protection Agency (EPA), 2017). The glyphosate levels in all surface water samples were below this MCL.

Moreover, when into the heavy-metals and residual pesticides found in the area, the remaining concentrations were negligible and far below the maximum allowed levels specified by WHO (Jayatilake, 2013; Nanayakkara et al, 2014).

Multifactorial Effect on CKDu

Some studies discuss the interaction between more than one component either synergistically or antagonistically affects CKDu (Dharma-wardena, 2017). According to the experiments conducted by Wasana et al. (2015), experiments have been conducted to check the multifactorial effect of As and , Cd and , Al and and hardness and on nephrotoxicity using mice. Despite all the multifactorial effects, the nephrotoxicity of hardness and Fluoride on nephrotoxicity had been identified by Dharmawardena (2018) as one of the crucial hypotheses on CKDu.

Existence of Hardness and Fluoride in water in CKDu prevalent areas

In Sri Lanka, most of the population in CKDu affected villages consumes groundwater acquired from the aquifers in the high-grade metamorphic regolith, which are mainly unstratified weathered or partly weathered loose rocks or soils. Estimates show that over 87% of the population in the dry zone regions of Sri Lanka use groundwater that is directly extracted from shallow wells of about 10 m depth or deeper wells with deep about 60 m (Dissanayake & Chandrajith, 2018; Panabokke, 2007). Many earlier studies on CKDu revealed that people who drink well water are more vulnerable to the disease when compared to those who consume water from public water supplies, natural springs, rainwater, and surface waters from reservoirs and rivers (Wasana et al., 2016). When considering the composition of spring waters, the hardness and fluoride values are comparatively low than the groundwater in CKDu prevalent areas (Wasana et al., 2015).

A distinct amount of fluoride is added into groundwater due to the regolith weathering of hard rocks (Dissanayake & Chandrajith 2018). The same phenomena are applied for the groundwater of the dry zone of Sri Lanka due to the leaching of mica, apatite like minerals rich in fluoride present in metamorphic rocks. The chemical similarities of hydroxyl and fluoride ions favor the leaching process (Saxena and Ahmed 2003). Even though there is no distinct difference of the lithology is in the dry zone and the wet zone, considerable differences of fluoride levels in groundwater were observed in the wet and dry zones with mean values of 0.33 mg/L and 0.76 mg/L, respectively in Sri Lanka. The facts behind the increased solute concentrations of hardness and fluoride in the dry zone of the country may be the concentrating of solutes due to the higher evaporation rate (Rubasinghe et al., 2015). The annual average rainfall is about 2500 mm and wells are more frequently flushed by frequent rains in the wet zone, leading to lower fluoride levels. This may explain the absence of CKDu in the wet zone of Sri Lanka

Even within small geographical distances of the NCP, the F^- distribution in groundwater is uneven and which is strongly vary over lateral distances of only a few tens of meters. A minimum distance between a high fluoride well (> 4.0 mg/L) and a low fluoride well

(< 1.5 mg/L) was 42 m (Ranasinghe et al., 2019). Besides, uneven distributions of F^- in groundwater in metamorphic terrains of Sri Lanka may explain the complex and mosaic distribution of CKDu in the dry zone region. Since the kidneys are among the main pathways of excreting fluoride from the body (Buzalaf et al., 2015), links between environmental fluoride exposure and CKDu need to be investigated in more detail.

2.5.1 The effect of Fluoride on CKDu

Fluoride can occur naturally in water above desirable levels. Fluoride contents above WHO recommended maximum limit (1.5 mg/L) have been reported in groundwater of NCP by Dissanayake and Weerasooriya (1985), Dissanayake (2005), Herath et al. (2005), Bandara et al. (2008), Perera et al. (2008), Chandrajith et al. (2010) and Dissanayake et al. (2012).

Ramseyer et al. (1957) and Cittanova et al. (1996) have shown damage to the kidney tissues from excessive and long-term exposure to fluoride. Furthermore, a dose-effect relationship between fluoride levels and CKDu has been reported as far back by Lantz et al. (1987). Recent animal-based studies have shown that kidney damage can occur after exposure to fluoride (Chattopadhyay et al., 2011; Niu et al., 2016). Controversially the experiments done by Wasana et al. (2015) have shown that there is no nephrotoxicity is shown when the mouse was exposed to 7 times of WHO MAL (1.5 mg/L x 7). To date, biological mechanisms that cause fluoride toxicity to the kidneys are poorly understood and other factors including water hardness (i.e., the sum of Ca^{2+} and Mg^{2+}) need to be considered.

The undesirable effects of fluoride on cellular systems have been investigated by Agalakova and Gusev (2012) which reveals that fluoride can induce oxidative stress, intracellular redox homeostasis, lipid peroxidation, protein synthesis inhibition, gene expression alteration, and apoptosis. Patients with reduced glomerular filtration rate have decreased ability to excrete fluoride in urine exposing them to increased risk of chronic fluoride toxicity (Schif, 2018). Fluorine is the most electronegative element. Due to its very high reactivity, fluoride is a marked geochemical reactant in

groundwater. A recent study by Dharma-wardana (2018) suggests F^- in the presence of Mg^{2+} hardness to be more nephrotoxic than fluoride ions alone.

2.5.2 Combined effect of Fluoride and Hardness

Magnesium and Calcium ions are the major cations that contribute to the hardness of the water in the NCP. One of the noteworthy features of the areas with CKDu in the dry zone of Sri Lanka is the high prevalence of water with high hardness often exceeding 75 mg/L (Chandrajith et al., 2011b) and high average fluoride levels with a mean value around 1.2 mg/L. The fact that these regions also superimpose, in many cases, on the high fluoride areas brings into focus a further complicating factor, and possibly both water hardness and fluoride play a role in the etiology of the kidney disease. Hard water, by itself, may not pose a serious threat to human health, but its main components, Ca^{2+} and Mg^{2+} may interact with other species to form complexes that may be of significance in health issues.

When such water with high fluoride levels is consumed in large quantities, as in the case of the dry zone population of Sri Lanka, the interactions of $Ca^{2+,}$ Mg^{2+}, and F^- may, in all probability, have an impact on the physiological functions. Dharma-wardena et al. (2015) suggest that while the increase of hardness (below a threshold) correlates with good health, ionicity increases above a threshold would correlate with ill health. Magnesium is the activator of more than 300 enzymes (Gröber, 2009), while fluoride is known to act as an inhibitor. Their geochemical and subsequent biochemical interactions are of importance in tracing the pathways to kidney disease. (Strochkova and Zhavoronkov, 1983).

According to Sauerheber (2013), ingested fluoride can form complexes with dietary calcium, and CaF_2 is formed. If fluoride exposure is sufficiently high or prolonged, the formation of kidney and gall stones is known to occur, due to the low solubility of calcium fluoride (at pH 7 at room temperature) (The Handbook of Chemistry and Physics, 50th edition, Chemical Rubber Co., Cleveland, Ohio, 1976). Further, as calcium fluoride is not soluble calcium ions can act as an antidote in fluoride poisoning. Based

on the experiments done by Wasana et al, (2017) it is seen that results of Wasana et al (2017) fluoride is not nephrotoxic even at 6.7 times of the MAL (i.e. 10 mg of F^- per liter of soft water) and it has become nephrotoxic in the presence of hard water when its present in MAL with hardness (1.5 mg/L,), and it has shown a higher nephrotoxicity even than cadmium is in soft water. Therefore, the synergistic interaction between fluoride and hardness on CKDu can be identified as a major causal factor for CKDu.

Moreover, the presence of heavy metals in groundwater, including frequently discussed Cd and As is very less and remained below WHO standards where the hardness and Fluoride concentrations in CKDu prevalent areas are above MAL of WHO standards.

The water is hard when its hardness is above 180 mg/L where the hardness of the water in CKDu prevalent areas is always above 180 mg/L always. According to Darma-wardana, (2017) the Gibbs free energy for ion-pairing between calcium ions and fluoride ion is positive no ion pair formation between calcium ions and fluoride ions can be expected. Thus, no toxic effect due to ion pair formation between fluoride and Calcium can be expected.

According to the experiments done by Wasana et al. (2015), the free energy change for magnesium ions to pair with fluoride ions to form $(MgF)^+$ ions is – 545 $KJmol^{-1}$. Thus, at the concentrations of Mg^{2+} and F^- specified by the experiment of Wasana et al (2017), some of the fluoride may be converted to the form $(MgF)^+$. According to Shigel (2019), in a 10 mg/L of a Fluoride solution, only 20% of Fluoride will be converted into MgF^+. The $(MgF)^+$ ion-pair looks like a Na^+ ion and it approaches a protein surface if the distance of approach is significantly larger than ~ 0.2 nm. At closer range, the Mg^{2+} and F^- will break apart under the electric fields of the ionic centers and H-bonding sites of the protein. The magnesium and fluoride ions are delivered to the wrong sites, e.g., possibly docking sites in epithelial Na-channels, disrupting their reactive capacity and structure. The divalent Mg^{2+} will also be delivered to the wrong sites. Hence fluoride ions in the presence of magnesium hardness may be expected to be more nephrotoxic

than fluoride ions alone and this has been experimentally proven by Wasana et al. (2015).

Therefore, removal of hardness and Fluoride levels in potable groundwater to a desirable level will be one of the solutions to control its interactions in potable water, and therefore it will be a solution to eliminate CKDu in the north-central province of Sri Lanka.

2.6 Defluoridation of Potable Water

Defluoridation techniques are applied to reduce the concentration of fluoride in the water to make it safe for human consumption. Some of the widely applying defluoridation techniques are including precipitation and coagulation, ion-exchange, membrane separation (reverse osmosis), electrodialysis, and adsorption (Bhatnagar et al., 2011; Habuda-Stanić et al., 2014; Meenakshi & Maheshwari, 2006; Renuka & Pushpanji, 2013)

2.6.1 Ion-Exchange

Commercially available synthetic anion resins are applied for the removal of fluoride from water. Generally, resins are packed in an Ion - exchange column, and fluoride-containing water is sent through the column.

The fluoride removal proceeds according to the following reaction:

$$\text{Matrix-DR3} + Cl^- + F^- \rightarrow \text{Matrix-DR3} + F^- + Cl^-$$

where DR3 is the cation exchange group. The F^- in the water is substituted by the chloride ion in the resins and the defluorinated water comes as eluent. (Khandare, 2013; Meenakshi & Maheshwari, 2006).

2.6.2 Adsorption

Adsorption technology is widely used to remove water-soluble ions from aqueous solutions, especially when these ions exist in low concentrations. Several studies have

been reported in the literature on the use of various adsorbents for fluoride removal from drinking water. The studies have mainly focussed to have alternative adsorbents that are low in cost, have local availability, require little processing, and are superior in performance. Synthetic adsorbents have good capacities for fluoride, but are always expensive, while natural materials that are available in large quantities from agricultural or industrial waste may potentially be low-cost materials (Onyango et al., 2006).

The adsorption of fluoride on a solid adsorbent usually occurs through three phases:

1. diffusion of fluoride ions to the surface of the adsorbent from the fluoride solution,
2. adsorption of fluoride ions on to particle surfaces,
3. the fluoride adsorbed on the surface will be exchanged with the relevant anion exchangeable elements inside the adsorbent.

Depending on the chemistry of the adsorbents, adsorbed fluoride ions will be transferred to the relevant internal surfaces (Salam et al., 2018).

Different synthetic and natural adsorbent materials have been utilized for adsorption. Some of them are Aluminum-based adsorbents, zeolite-based adsorptions, carbonaceous materials-based adsorptions, and synthetic resins-based adsorbents.

2.6.3 Membrane separation (RO and Electrodialysis)

RO is an expensive technique where; a pressure is applied to the water to move it through a semipermeable membrane while leaving fluoride ions and its related salts behind. (Renuka & Pushpanji, 2013).

2.6.4 Precipitation and coagulation technique

The addition of coagulant and coagulant aids to precipitate sparingly soluble salts of fluoride is done during the coagulation and precipitation process. Nalgonda technique is widely using coagulation and precipitation techniques for defluoridation in developing

countries including India, Kenya, Senegal, Tanzania, and rural China (Bhatnagar et al., 2011)

Table 2.1: Available defluoridation methods in the absence of other ions with advantages and limitation

Defluorination method	Limitation	Advantage	Reference
Adsorption	Highly pH and temperature-dependent.	Cost-effective Can remove more than 90% of fluoride with some adsorbents, Economical, operation is easy, no high pressure is required	Liu et al., 2005; Zhao et al., 2017
Ion exchange	Retains the superiority of water.	High productivity (90-95 % fluoride removal).	AMansur Zarrabi, 2014; Graeme et al., 2017
Membrane filtration	Expensive technique, Membrane can be	Productivity is high. It can be used under a	Assefa et al., 2009; Pontie et al., 2008)

	damaged due to fouling and scaling	wide pH range. Interference due to the presence of other ions is not reported	
Coagulation/precipitation: calcium hydroxide; aluminum hydroxide	Expensive Efficiency controls by pH and the presence of other ions pH must be adjusted	High efficiency: Required chemicals are commercially available	Gohary et al., 2010; Gong et al., 2012

Most of the above methods are responsible for removing fluoride from the water are expensive and secondary waste is accumulated in some techniques (Loganathan et al., 2013). Therefore, less expensive and non-secondary waste generating methods are to be employed for the removal of the excess amount of fluoride from drinking water. Based on the above criteria, the absorption-based process provides a large number of favorable properties including, simplicity, higher effectiveness and efficiency, and low cost (Ganvirand et al., 2011). The various absorbents are utilized for removing fluoride namely activated alumina (Jagtap et al., 2011), activated carbon (Zhao et al., 2012), mixed metal oxides (Zhao et al., 2012), clays (Karthikeya et al., 2005), industrial wastes (Wu et al., 2013), zeolite (Z. Zhang et al., 2011).

Table 2.2: Different adsorbents used for defluoridation

Adsorbent	Q_e mg/g	pH	Temperature	Reference
Aluminum Based Adsorbents				
Acidic alumina	8.4	4.4	25	Goswami and Purkait (2012)
Aluminum alkoxide	240.6	7	30	Kambleetal (2010)
AIAA		6.5	25	Tripathy et al. (2006)
MAAAA	10.1	5-7.5	30	Mlaiyekkal et al. (2008)
MCAA	1.2	7	25	Tripathy and Rachiur (2008)
Al - Ce based adsorbent	27.5	6-7.5	25	Liu et al. (2010)
Ti-Al metal oxide	2.2		27	Thakre et al. (2010)
Al (OH)3 coated AC	22.7	7	27	Amalrajet al. (2016)
MIAA	0.7		20	Rafique et al. (2012)
Calcium Based Adsorbents				
Charcoals containing Al	19.5	7	25	Tchomgui - Kamaga et al. (2010)
CA	43.1		25	Sakhare et al. (2012)
Eggshell composite	37	6	30	Lunge et al. (2012)
Glass derived HAP	17.3	6.7	35	Liang et al. (2011)
Al-HAP	32.5	5	25	Nile et al. (2012)
Carbon Based Adsorbents				
Carbonaceous material	2.84	7		Mendoza et al. (2012)
CeDC	29.1	7.7	25	Sivasaker et al. (2013)
Bark of babool	0.7	7	30	Mamilwae et al. (2012)
Neem Charcol	18.8	5	30	Chakrabarty et al. (2012)
MB	2.2	9	30	Thakre et al. (2010)

The defluoridation ability of natural zeolites is high while it is comparatively high in coal-derived fly ash (q_e = 0.8mg/g) (From this study)

Some Authors including Sudsinghe et al. (2019) and Kodikara et al. (2015) have focused on defluoridation in hardness using electrodialysis and adsorption using zero-valent ion respectively where the research focusing on defluoridation in the presence of hardness is poor.

2.7 Use of Coal Fly Ash (CFA) derived Zeolites as a low-cost adsorbent for Defluoridation

Zeolites are a naturally occurring mineral where also commercially produced on a large scale. They are hydrated aluminosilicate frameworks with pores that are occupied by water and some earth metal cations. They can be utilized as adsorbents due to their porous structure. Moreover, Zeolites can be used as a cation exchanger due to the presence of a net negative charges over a large surface area (Wang et al., 2010). Their affinity towards anions is less due to the presence of a net negative charge and therefore zeolite does not work as a good anion adsorbent (Nasser et al., 2012).

Natural zeolites are formed when volcanic rocks and ash layers react with alkaline groundwater (Dypayan, 2007). They are not pure always have been contaminated with some minerals, metals, quartz, etc, where the chemical composition, size of the crystal, the diameter of the pores are the crucial factors that determine their sorption and ion exchange capacity (Lydon, 2013).

Zeolites can be synthesize using silica and alumina bearing raw materials by alkali treatment. The raw materials can be by-products and wastes of some manufacturing processes such as coal fly ash, municipal solid waste incinerated ash, rice husk ash (Lydon, 2013).

Coal fly ash (CFA) is one of the most abundant by-products ultimately filled in open dumps as a waste through the coal combustion process. Norochcholei coal power plant in Sri Lanka produces approximately 150 metric tons coal of fly ash per year and only

20% of them are used for cement production, and the rest is disposed of as open dumping causing severe social, economic, and environmental hazards to the normal life of the people living in the area (Venuja et al., 2017). Coal fly ash can be converted to usable zeolite with the hydrothermal method for modifying its chemical and physical properties including functional groups, porosity, crystallinity, and surface area (Lydon, 2013). Moreover, further modifications can be done to develop zeolite as an adsorbent to improve its function as an adsorbent (Ertan et al., 2005). The adsorption capacity can be raised by changing the surface of the salt with the cationic surfactants or the metal cations (Samatya et al., 2007).

Different metal oxides have been used for the modification of zeolites for defluoridation including Al, Mg, Ca oxides (Sanghratna et al., 2015; Devi et al., 2014; Xu et al., 2008). When Na^+ in zeolite is exchanged with metallic ion like Fe^{3+}, its active sites are generated for fluoride adsorption. The properties such as small size, hard base nature, high electronegativity makes the fluoride compatible with metal ions (S. Xingbin et al., 2010). Chemical modification with inorganic salt like $FeCl_3$, $Mg(NO_3)_2$, $Ca(NO_3)_2$ gives to improve zeolite properties and increase its efficiency in water treatment (Kumar et al., 2009; Li Z et al., 2007).

Modification of Zeolite surfaces with an inorganic salt solution having a high concentration is ideal for a proper surface modification. To remove anions such as fluoride from the water, the zeolite surface has to be modified with a concentrated solution of inorganic salts like $FeCl_3$, whose adsorption on the zeolite surface leads to the formation of oxi-hydroxides, which then form stable complexes with anions in solution. This modification can result in a smaller or greater extent in the creation of an adsorption layer on the zeolite surface and modification of surface charge on zeolite.

2.7.1 Modification of MFA with Iron oxide

Modification of MFA can enhance its positively charged sites. Some of the modifications done on MFA for defluoridation are given in *Table 2.3*.

Table 2.3: Defluoridation when MFA is modified with different components

Fly Ash modification	q_e (mg/g)	Reference
Fly Ash only	0.30	Chaturved et al. (1989)
CaO and Al_2O_3	0.45	Perera. (2019)
Paper mill lime mud	7.37	Changwen Ye et al. (2019)
Al_2O_3	3.40	Goswami et al. (2005)
Fe_2O_3 and Fe_3O_4	10.00	This Study

2.7.2 Importance of Modifying MFA with Fe

Fe remains in Fe^{2+} or Fe^{3+} cationic forms in aqueous solution and they are capable of formation of Fe_2O_3 and Fe_3O_4 during oxidation.

Chemical modification with inorganic salt like $FeCl_3$ gives to improve zeolite properties and increase its efficiency in water treatment (Kumar et al., 2009; Liz et al., 2007). Fe^{3+} ions can enter empty zeolite cavities and replace balancing cations in interchangeable zeolites.

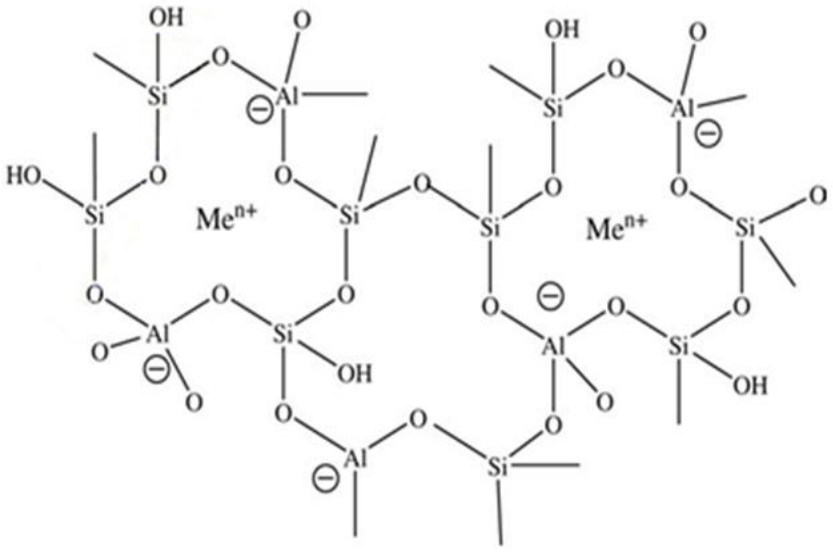

Figure 2.3 Schematic illustration of negatively charged MFA surface (Mohau et al., 2017)

Fe^{3+} and Fe^{2+} oxide forms can easily bind with negatively charged MFA providing MFA a positive charge. , (ionic radius 136 pm) is similar to that of the hydroxyl (OH^-) ion (ionic radius 140 pm) and highly electronegative, hence there can be easily exchanged between them (Dissanayake, 2019). The pore diameter of MFA is larger than that of the ionic radii of Fe^{3+} and Fe^{2+} (Baiber et al., 1972), thus Fe ions can further penetrate inside of the porous MFA structure Further, Fe^{3+} is no toxic metal like Al, hence has no health hazard thus can be used for drinking water treatment. Very few experiments have been done to study the defluoridation effect of Fe^{3+} alone (Jayarathne et al., 2015) where no research has been done on the defluoridation capacity of $FeCl_3$ functionalized MFA.

2.8 Mechanism of impregnation of Fe into MFA

The presence of a negative charge on the P Zeolite (MFA) structure, causes to have a small ability of MFA to adsorb anion. Therefore, modification of zeolite to improve the anion exchange properties can be done by modification of MFA with transition metal cations such as Fe (III). Ion Fe (III) can enter empty zeolite cavities and replace balancing cations in interchangeable zeolites (Danabas et al., 2011). Then MFA is capable to adsorb the anions (Hamdan et al., 1992).

Protons from the acidic zeolite OH^- groups in MFA can be replaced with Fe atoms while on MFA structure. The process is strongly exothermic, −384 kJ/mol, and spontaneous. During the redox reaction, protons in MFA are reduced to H_2, while Fe atoms are oxidized to Fe^{2+} cations which compensate the negative charges around both Al centers. Moreover, Fe^{3+} ions in solution can replace protons from the OH^- groups in zeolite too. ZEO/Fe^{2+} structure can be formed during this ion exchange (neutralization) from the protonic form of the MFA, $ZEO/2H^+$, by $Fe^{2+}(OH)_2$. The process is exothermic and −145 kJ/mol (Senamart et al., 2019). When a higher loading of Iron occurs, Iron oxide clusters in the zeolite pores can be formed. This Iron oxide is converted to Iron hydroxides during hydration (Gurgul et al., 2013).

3 MATERIAL AND METHODS

3.1 Establishment of the distribution of fluoride and hardness levels present in potable water in CKDu affected and non-affected areas

Secondary data on the hardness and fluoride concentrations in potable water of the CKDu prevalent areas and non-prevalent areas were collected from the reports available at the Water Resources Board and also published literature. These data were analyzed to identify the correlation between the hardness and fluoride levels present in potable water with the CKDu prevalence. The water quality data gathered are presented in Annexure 1.

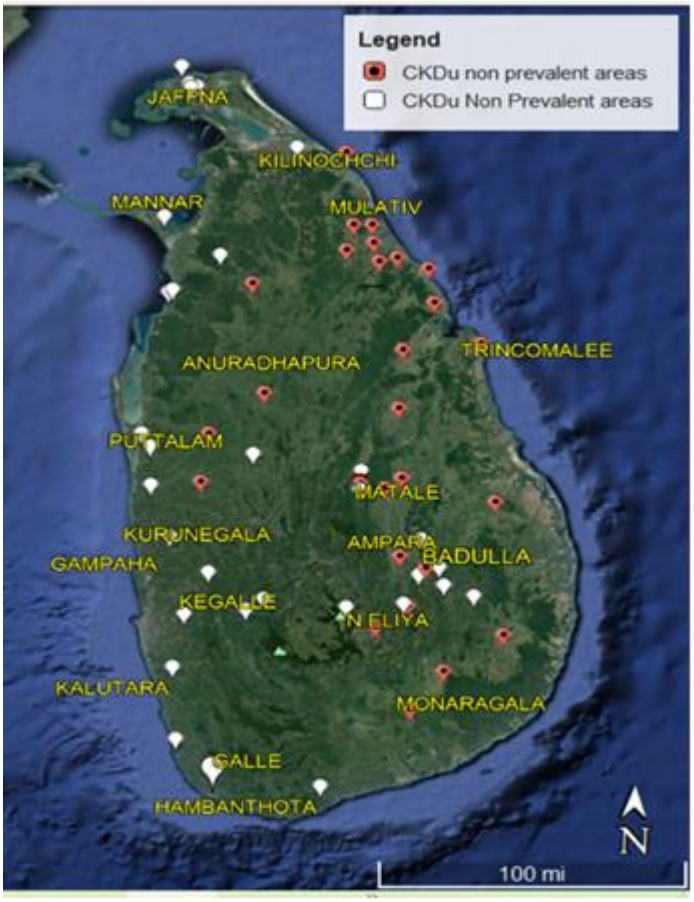

Figure 3.1 The regions selected to study the hardness and fluoride levels distribution in potable groundwater in Sri Lanka

3.2 Development of an ion-exchange column to remove hardness to a desirable level for an enhanced defluoridation

The synergistic effect of Hardness and fluoride has been identified as one of the major causal factors for CKDu. Based on the data gathered, it was noted that the hardness levels are higher (From 150 — 600 mg/L) in the CKDu prevalent areas compared to the CKDu non-prevalent areas (from 30-300 ppm). Water containing high hardness is not pleasant to drink. Also, the defluoridation efficiency of the adsorbent materials can be reduced due to the adsorption of Ca^{2+} and Mg^{2+} ions from the water. Further, at low hardness levels, the concentration of Mg^{2+} and Ca^{2+} ions would also be low (Ca^{2+}: Mg^{2+} ratio = 1:4) and it is anticipated that low interaction of Ca and Mg with F will occur. Thus the synergistic effect due to hardness and fluoride on nephrotoxicity can be overcome. Therefore, as the first stage of the study, the removal of hardness to a desirable level was found to be important to minimize the interference of hardness on defluoridation by the adsorbents.

An ion-exchange column was developed exclusively for the removal of hardness before focusing on defluoridation of the water**.** A divalent cation exchange column was developed with the aid of divalent cation resin (Eco 1, specification is attached in Annex 2). The height, diameter, and the total volume of the constricted cation exchange column are 4.50 cm, 3.00 cm, and 31.79 cm^3 respectively. The hydraulic retention time (HRT) and the flow rate of incoming water were 2.00 minutes and 16 ml/min respectively. The synthetic solution prepared to contain 600.00 mg/L of hardness and 2.60 ppm of fluoride was continuously pumped through the prepared column using a peristaltic pump at a flow rate of 16 ml/min. The eluent was collected, and the hardness level of the eluent was measured every 30 minutes. A with the aid of EDTA using EBT as the indicator given in Betz et al. (1950). The breakthrough curve for the prepared ion exchange column was developed and the maximum operating time for the ion exchange column was calculated with the aid of a breakthrough curve for the constructed ion exchange

column. (The calculations related to the design of ion exchange column is given in Annex 3)

Based on the breakthrough curve developed, the ion exchange column was operated until the eluent hardness concentration is 200 mg/L. The apparatus of the constructed ion exchange column is given in Figure 3.2.

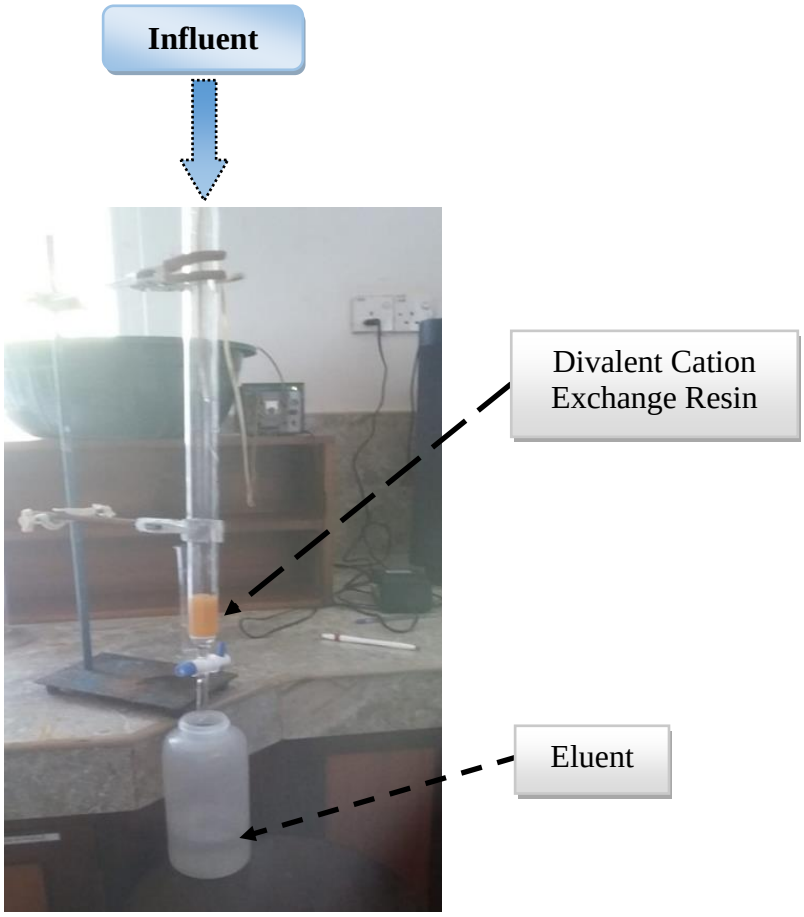

Figure 3.2 Ion exchange column set up

3.3 Defluoridation using functionalized modified Fly Ash

Based on the secondary data on Fluoride and hardness (Annex 1), the synergic effects between hardness and fluoride on CKDu were minimal when the fluoride level was 0.47ppm and hardness is 200.00 mg/L. Hence, in the second stage of the study, the

eluent of the ion exchange column was further treated using Ion oxide Functionalized Modified Fly Ash (FMFA) to remove the excessive fluoride up to 0.47 mg/L to minimize the CKDu risk.

3.3.1 Synthesis of Coal Derived Modified Fly Ash (MFA)

Coal fly ash (CFA) obtained from Norochcholey Coal Power Plant was soaked in 10% Nitric acid for 24 hours to remove impurities in fly ash. Then it was washed with distilled water until the pH of the fly ash reaches to pH 4 to have a better functionalization. Then it was dried in an oven at 60 °C for 12 hrs. Later, the modified Fly Ash was synthesized by mixing a known amount of dry fly ash (140 g) with 2M NaOH (350 ml) and refluxed at 90 ^{o}C for 96 hours (Molina et al., 2004). After that, the mixture was filtered and washed three times with DI water and dried at 70 ^{o}C for 24 hours (Molina et al., 2004). The procedure for synthesizing coal-derived MFA is given in Figure 3.3.

Experimental procedure for the synthesis of Modified Fly Ash (MFA)

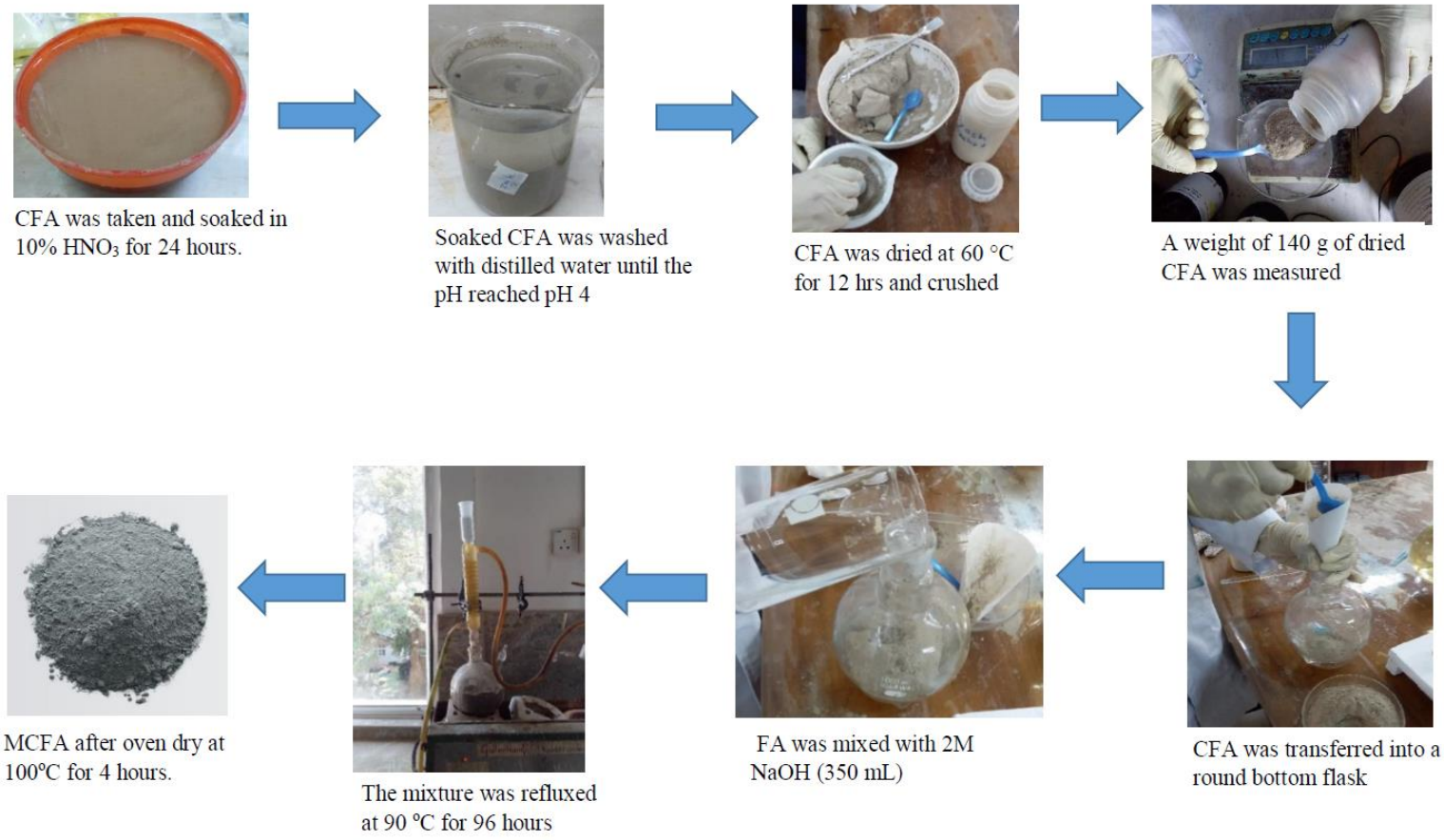

Figure 3.3 The procedure for synthesize of MFA from coal derived fly ash

3.3.2 Synthesis of Ion Functionalized MFA(FMFA)

The method described by Petala et al. (2013) was further modified for the synthesis of Fe modified MFA. In every batch of synthesis, predetermined weights combinations of $FeCl_3.6H_2O$ and MFA as given in *Table 3.1* and 0.50g of Polyethylene glycol were dissolved in a 100.00 mL of 75% CH_3CH_2OH. The prepared solution was stirred on a magnetic stirrer and compressed nitrogen gas was purged at a rate of 3.5 L/min through the above-prepared solution for 24 hours. 1000.00 mL of 0.33M Sodium borohydride solution was prepared and added dropwise to the solution containing Fe^{3+} and MFA with the aid of a burette while stirring the mixture on the magnetic stirrer. The pH of the solution was maintained at 7 using an ammonium hydroxide solution. After completing the addition of Sodium borohydride solution, the mixture was left for another 15 minutes to stirrer. The prepared FMFA was separated from the liquid phase using 50% ethanol by sonicating 15 minutes and followed by centrifuging at 300 R.P.M and rinsing thrice times in 95% ethanol. The obtained product was oven-dried at 80 °C (Gui et al., 2012). Finally, the product was calcified at 450^{o}C. The calcified Ion oxide Functionalized Modified Fly Ash (FMFA) was crushed into small particles and stored in glass tubes.

Table 3.1 Mixing weight ratios of FeCl3.6H2O and Fly Ash

Weight ratio of MFA: $FeCl_3$		
	MFA	**$FeCl_3$**
FMFA1	1	1
FMFA2	2	1
FMFA3	3	1
FMFA4	1	2
FMFA5	2	3

12 g of $FeCl_3$ dissolved in 500 ml of Deionized water and 12 g of MFA was added and stirred for overnight under 100 rpm

1.00 L of 0.1M Sodium borohydrate and 25 ml of conc ammonia solution was added while shaking at 100 rpm

Prepared mixture was washed with ethanol and centrifuged to remove water

Sonication was programmed to high intensity with normal pulse at 70 ^{0}C for 90 minutes

Oven dried for an overnight at 60 ^{0}C

Final Crushed Functionalized Modified Fly Ash (FMFA)

Figure 3.4 Procedure for the synthesis of $(FMFA)_{opt}$

3.4 Characterization of synthesized MFA and Coal Fly Ash (CFA) using SEM, EDX, XRD, and FTIR

The synthesized FMFA, MFA, and CFA were analyzed for the morphology and elemental composition with the aid of Environmental Scanning Electron Microscopy (ESEM- Carl Zeiss, EVO 18, Secondary Electron Microscope, Germany) coupled with Energy- Dispersive X-ray Spectroscopy (EDX Z1 analyzer, USA).

The phase identification of the Zeolite was performed by the X-ray Powder Diffraction (XRD-D8, ECO, Advance Bruker Diffractometer with filtered Cu Kα radiation, Germany). Fourier Transform- Infrared Spectroscopy (FTIR, ALPHA Bruker, Germany) was performed in the adsorption mode at ambient temperature in the spectral range of 500–4,000 cm^{-1} to identify the functional groups of the Zeolite.

3.5 Characterization of $(FMFA)_{opt}$ and MFA using SEM, EDX, XRD, and FTIR

The morphology and elemental composition of MFA and $FMFA)_{opt}$ were analyzed using Environmental Scanning Electron Microscopy (ESEM- Carl Zeiss, EVO 18, Secondary Electron Microscope, Germany) coupled with Energy-Dispersive X-ray Spectroscopy (EDX Z1 analyzer, USA). X-ray Powder Diffraction (XRD-D8, ECO, Advance Bruker Diffractometer with filtered Cu Kα radiation, Germany) used for phase identification. Functional groups in MFA and $(FMFA)_{opt}$ were identified with the aid of Fourier Transform-Infrared Spectroscopy (FT–IR-ATR, ALPHA Bruker, Germany), and it was performed in the adsorption mode at ambient temperature in the spectral range of 500–4,000 cm^{-1}. The chemical and physical changes that happened on MFA, during modification was studied.

3.6 Evaluation of the defluoridation efficiency for different combinations of $FeCl_3$ and FMFA

Batch experiments were carried out using FMFA1-FMFA5 and MFA to study the fluoride adsorption. Anhydrous NaF, $Mg(NO_3)_2$, $Ca(NO_3)_2$ (from Merck, Darmstadt, Germany) were used to prepare hardness (Ca + Mg hardness), and fluoride solutions.

Analytical grade reagents were used throughout the experiment. The fluoride removal was studied with a solution containing 2.00 mg/L of fluoride concentration and 200 mg/L of hardness concentration (Ca and Mg Hardness) with (Ca: Mg 4:1 as prevail in CKDu areas) for 1.0g of above-prepared series of FMFA and 1.00g of raw modified fly ash in 100 ml of pre-prepared and filtered hardness and fluoride-containing solution for 24 hours of contact time.

When considering the effect of other anions present in potable waters of CKDu prevalent areas**,** Cl^- is the dominant anion present where the anionic concentrations vary as $Cl^- > SO_4^{2-} > F^- > NO_3^- > PO_4^{3-}$ in groundwater of CKDu prevalent areas (Cooray et al., 2019). During the experiments of Chai et al. (2015), they have observed that there was no effect on adsorption of fluoride due to the presence of Cl^-, SO_4^{2-} and NO_3^-. Further the electronegativity of chloride ions (3.16) is lesser than the electronegativity of that of fluoride ions (4.00) (Gupta, 2016). Therefore, fluoride ions have more affinity towards adsorption onto the adsorbent. The pH was maintained between 6.0 and 7.0. The residual fluoride concentration was measured using the Ion Chromatography (930 compact IC Flex1) using a mobile phase with 4 mM Sodium carbonate and 1.25 mM Sodium bicarbonate. The material given the required fluoride removal (Removal of fluoride below 0.47 mg/L was identified, and it was named as $(FMFA)_{opt}$.

Figure 3.5 The experimental set up for batch experiments

3.7 Characterization of FA $(FMFA)_{opt}$ using SEM, EDX, XRD, and FTIR

The morphology and elemental composition of Fluoride adsorbed optimized Functionalized Modified Fly Ash $(FAFMFA)_{opt}$ was analyzed using Environmental Scanning Electron Microscopy (ESEM- Carl Zeiss, EVO 18, Secondary Electron Microscope, Germany) coupled with Energy-Dispersive X-ray Spectroscopy (EDX Z1 analyzer, USA). X-ray Powder Diffraction (XRD-D8, ECO, Advance Bruker Diffractometer with filtered Cu Kα radiation, Germany) used for phase identification. Functional groups in FA(FMFA)opt were identified with the aid of Fourier Transform-Infrared Spectroscopy (FT–IR-ATR, ALPHA Bruker, Germany), and it was performed in the adsorption mode at ambient temperature in the spectral range of 500–4,000 cm^{-1}. The chemical and physical changes that happened on (FMFA)opt after adsorption of fluoride was studied.

3.8 Optimization of experiment condition for the (FMFA) opt for defluoridation

A water sample containing 200.00 mg/L of hardness and 2.00 mg/L of fluoride was prepared by dissolving calculated weights of analytical grade $Ca(NO_3)_2$, $Mg(NO_3)_2$, and NaF respectively in deionized water. The Ca^{2+}: Mg^{2+} ion ratio of the solution was kept 4:1 as in the water of CKDu prevalent areas and the synthesized water was applied for further defluoridation experiments, isotherm studies, and kinetic studies. Batch experiments were conducted to find the optimum dosage, contact time, and pH of FMFA to have the highest effective defluoridation.

3.8.1 Selection of the optimum FMFA dosage

Different weights of $(FMFA)_{opt}$ to range from 0.05 g to 2.00 g were added to 250.00 mL conical flasks containing 100.00 ml of the above-synthesized solution containing 200.00 mg/L of hardness and 2.00 mg/L of fluoride and kept them to mix under 100 rpm on a mechanical shaker for 24 hours. The pH of the synthesized solution was adjusted to 6.00 and the experiment was done in a normal room temperature of 28 C. The dosage which could get the maximum defluoridation efficiency was selected as the $(FMFA)_{opt}$ and used for further experiments. The set up for the defluoridation batch experiment is given in Figure 3.5.

3.8.2 Selection of the optimum contact time

Each of 1.30g of $(FMFA)_{opt}$ were added into 10 conical flasks contained with 100 ml water with hardness (Ca2: Mg 4:1ratio, 200 ppm) and Fluoride (2 ppm) and kept for different time intervals from 0.00 minutes to 2.00 hours while shaking under 100 r.pm in the mechanical stirrer to determine the optimum contact time for defluoridation. The pH was adjusted as 6 and, the temperature was 28 ºC. The contact time given the maximum absorbance of fluoride was selected as the optimum contact time.

3.8.3 Optimum pH

100.00 ml of the synthesized solution containing hardness 200.00 ppm and fluoride 2.00 ppm were used for the optimum pH selection with the optimum dosage of $(FMFA)_{opt}$ (1.3g) and for an optimum contact time of 40 minutes of mixing time on a mechanical shaker.

The contact pH of the mixture was changed from pH 2 to 12 using 20% HCl and 20% NaOH. The pH value giving the maximum absorbance of fluoride was selected as the optimum pH.

3.9 Adsorption Isotherm and Kinetic studies for fluoride removal

Studies on Adsorption isotherms and kinetic models are of utmost importance in the adsorption process. Adsorption isotherm analysis helps to know whether the adsorption process is favorable, how much of adsorbate is adsorbed on the adsorbent, the mechanism of adsorption (whether a monolayer or a multilayer adsorption) whether the adsorption mechanism is favorable, etc. The adsorption data at the equilibrium were tested to check its fitness with the adsorption isotherm models including the Langmuir adsorption isotherm model and Freundlich adsorption isotherm model.

Moreover, thermodynamic studies were carried out to know whether the reaction is spontaneous or not, (Salameh et al., 2010).

The amount of fluoride removed per unit mass of $(FMFA)_{opt}$ in the equilibrium (Q_e in mg/g) for a single solute was calculated using Equation 1.

$$Q_e = (C_o - C_e) \times \frac{V}{W} \qquad (1)$$

Where C_o and C_e are the initial and the equilibrium concentrations of fluoride in the solution (mg/L) respectively, *V* is the volume of solution (*L*), and *W* is the mass of the adsorbent (g).

The adsorption of fluoride on FMFA was studied for Langmuir isotherm model and Freundlich isotherm model.

3.9.1 Langmuir Isotherm Model

The Langmuir adsorption isotherm model was applied used to study the nature of defluoridation and the amount of adsorbate adsorbed per unit weight of adsorbent in the equilibrium and to know whether the adsorption process is favorable. The model has some assumptions including that the adsorbent surface is homogeneous with equal sorption sites, only monolayer adsorption occurs with no interaction between adjacent adsorbed ions. Langmuir adsorption isotherm (Langmuir, 2018) is given by Equation 2.

$$\frac{1}{Q_e} = \frac{1}{Q_m} + \frac{1}{Q_m K_L C_e} \qquad (2)$$

Where C_e is the equilibrium concentration of adsorbate (mg/L), Q_e is the amount of adsorbate adsorbed per unit weight of the adsorbent at equilibrium (mg/g), Q_m is maximum monolayer coverage capacity (mg/g). The separation factor, R_L is given in Equation 3; where C_o is the initial concentration (mg L^{-1}), and K_L is Langmuir isotherm constant. R_L value can be used to predict whether the reaction if favorable or not. If the R_L value lays at ($0 < R_L < 1$), the defluoridation with the synthesized material is favorable. (Weber and Chakravorti, 1974).

$$R_L = \frac{1}{[1+(1+K_L C_o)]} \qquad (3)$$

3.9.2 Freundlich isotherm model

Freundlich isotherm model was applied to study the adsorption of fluoride with $(FMFA)_{opt}$. Following assumptions considered in the Freundlich isotherm model

1. Presence of heterogeneous surfaces to bind the adsorbate as a multilayer

2. Interactions between adsorbed ions

Freundlich adsorption isotherm (Freundlich, 1906) is given below in Equation 4.

$$\log(Q_e) = \log(K_f) + \frac{1}{n}\log(C_e) \quad (4)$$

Where K_f is the Freundlich isotherm constant (mg/g), n is the adsorption intensity, C_e is the equilibrium concentration of adsorbate (mg/L), and Q_e is the amount of adsorbate adsorbed per gram of the adsorbent at equilibrium (mg/g). The Freundlich constant (n) indicates the adsorption mechanism and when $2 < n < 10$, adsorption is favorable, between $1 < n < 2$ moderately difficult and $n < 1$ poor adsorption (Kakavandi et al., 2013).

3.10 Kinetic studies

Kinetics of fluoride adsorption were analyzed using Lagergren's pseudo-first-order kinetic model (Yuh-Shan, 2004), and the pseudo-second-order model (Ho and McKay, 1999). The adsorption of one ion of adsorbate to one adsorption site is considered in a pseudo-second-order kinetic model where adsorption of one ion of adsorbate to two adsorption sites is considered in the pseudo-second-order model (Ho and McKay, 1999). These two models were used to identify whether the kinetics of fluoride adsorption processes to be fitted to chemisorption or physisorption. The pseudo-first-order kinetic model and the pseudo-second-order kinetic models are expressed in Equation 5 and 6 respectively.

$$log(Q_e - Q_t) = \log Q_e - \left(\frac{K_1}{2.303}\right)t \quad (5)$$

$$\frac{t}{Q_t} = \frac{1}{[K_2\,(Q_e)^2]} + \left(\frac{1}{Q_e}\right)t \quad (6)$$

Where Q_e is the amount of adsorbate adsorbed on adsorbent (mg/g) at equilibrium, Q_t is the amount of adsorbate adsorbed on adsorbent (mg/g) at time t (minutes), K_1 is the

constant (min^{-1}) for pseudo-first-order kinetics, and K_2 is the rate constant (gm/g/min) for pseudo-second-order kinetics.

3.11 Regeneration studies for $(FMFA)_{opt}$

The regeneration of an adsorbent is of utmost importance to reduce the capital for material synthesizing and to minimize the accumulation of more waste. Experiments were carried out to check the regeneration ability of fluoride adsorbed material using acidic, basic, and neutral pH values with the aid of HCL, EDTA, and NaOH solutions with pH 4, 7, and 12, respectively to check the functionalization of the fluoride adsorbed material at acidic, basic and neutral medium to utilize it to remove fluoride again.

The batch experiments were conducted using 1.3g of $(FMFA)_{opt}$ in 100 mL of fluoride solution containing 2.00 ppm of fluoride and 200.00 ppm of hardness. The experiment was kept for 40 minutes to adsorb fluoride at 6.8 pH with continuous shaking on the mechanical shaker under 100.00 rpm. After the adsorption cycle $(FMFA)_{opt}$ was let to settle and the supernatant was decanted and filtered. The residual fluoride concentration in the supernatant was analyzed with the aid of the IC. 50 ml from above discussed each regeneration reagents were added to flasks with $FA(FMFA)_{opt}$ and kept them to be mixed homogeneously on the mechanical shaker at 100 rpm for an hour. The regeneration reagent was decanted and the remaining $FA(FMFA)_{opt}$ particles were washed with DI water thrice and the supernatant water was decanted. The conical flask contained $FA(FMFA)_{opt}$ was kept in the oven till a constant weight was achieved. The weight of the flask was recorded and then the above procedure was repeated for another two adsorption, desorption cycles. The weight change of the adsorbent after each regeneration cycle was minute (less than 0.05 g).

4 RESULTS AND DISCUSSION

4.1 Establishment of the Relationship between Hardness and Fluoride present in groundwater with the CKDu Prevalence

Based on the published literature, the hardness and fluoride concentrations of potable groundwater in different geographical locations (both CKDu prevalent and non-prevalent) in Sri Lanka were collected and presented as a scatter plot in Figure 4.1. The reported values on hardness and fluoride concentrations in CKDu prevalent areas and CKDu non-prevalent areas are presented in Annexure 1.

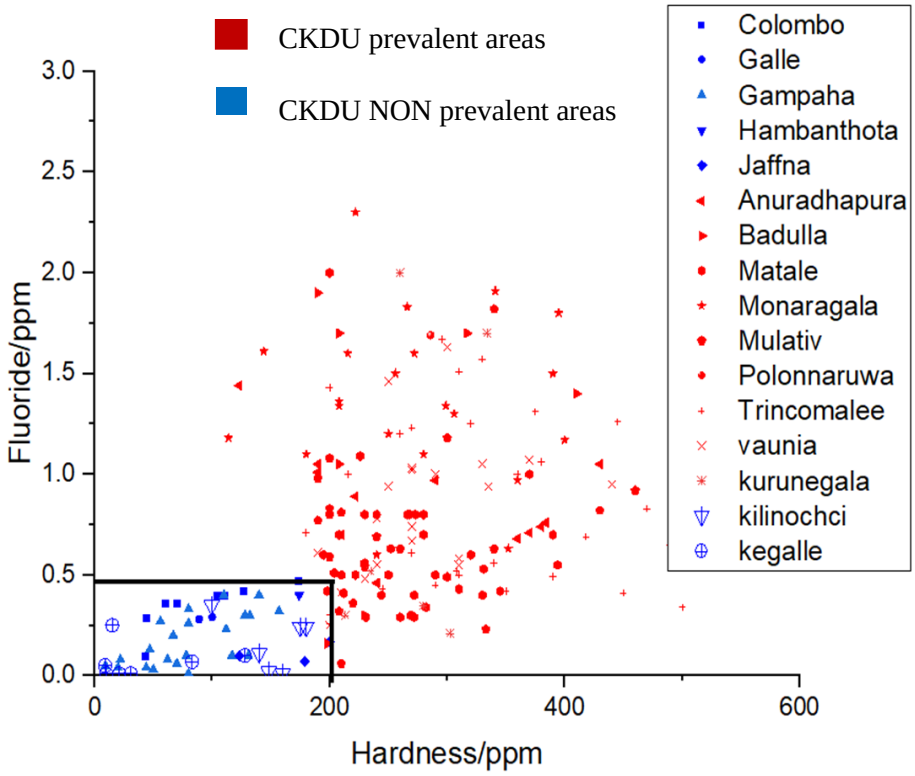

Figure 4.1 The hardness and Fluoride concentration in different geographical locations in Sri Lanka

The rationale in establishing the linkage between fluoride and Hardness was based on the ninety-five percentile values of reported Fluoride and Hardness values in the CKDu prevalent and non-prevalent areas. Any value reported below such percentile values in CKDu non-prevalent areas are presumed to be levels that are not susceptible to instigating CKDu.

Figure 4.1 presents the concentrations of hardness and fluoride in potable groundwater in different geographical regions in Sri Lanka. In Figure 4.1, each location marked in red represents the Hardness and Fluoride level of a particular CKDu prevalent location where icons marked in blue represents the hardness and fluoride levels of each CKDu non-prevalent locations.

On the scatter-plot in Figure 4.1, at 95% percentile values for hardness and fluoride in CKDu non-prevalent areas are lying below 200.00 ppm and 0.47 ppm in potable ground waters respectively. Hence this study presumes that, from a combination of hardness and Fluoride in non-CKDu prevalent areas, any combination below the ninety-five-percentile value would be considered as safe. Therefore, for further studies of this research, effective treatment methods were investigated to reduce the hardness level below 200.00 ppm and Fluoride level below 0.47 ppm for a safe consumption.

There are no nephrotoxic levels established for Fluoride and hardness. Hence, this study attempted to establish a hypothesis to show the linkage between Hardness and Fluoride as the causal agent for triggering CKDu

4.2 Use of a cation exchange column for the removal of excessive hardness levels in the presence of fluoride

Excessive hardness plays a crucial role in the water of CKDu prevalent areas. Based on the categorization of hardness levels, all waters in CKDu prevalent areas belong to the hard water category. Hard water has been classified in general water as soft (0–60 ppm), moderate (61–120 ppm), hard (121–180 ppm), and very hard (>180 ppm) (United States Geological Survey, 2009).

Therefore, reducing excessive hardness up to a desirable level may help to make drinking water pleasant. Further, as discussed above, the synergistic effect between water hardness and fluoride was observed. To eliminate this effect, hardness and fluoride concentrations in potable water need to be lowered until there would not be any nephrotoxic effect. Based on the rationale developed above, hardness below 200.00 ppm and fluoride below 0.47 ppm, no nephrotoxicity in drinking water was observed. Hence, before removing excessive fluoride from potable water, removal of hardness is done with the aid of a divalent cation exchange column.

4.2.1 Development of the breakthrough curve for the ion exchange column to remove excessive hardness

A synthetic commercially available resin (ECO A bought from Ecosoft Water Systems GmbH), which is exclusively developed for the exchange of divalent cations was used in the experiments. The water containing hardness 600.00 ppm and Fluoride 2.60 ppm was continuously pumped through the ion exchange column for 29 hours.

These hardness and fluoride levels were chosen based on the maximum hardness and fluoride levels present in CKDu prevalent areas as given in Figure 4.1.

The eluent was collected in every 30 minutes and remaining hardness and fluoride levels were measured. The hardness was analyzed using the titrimetric method with EDTA using EBT as the indicator. The minimum detection level of EDTA titration for hardness is 0.05mg/L. Only hardness removal was observed in the eluent as shown in Figure 4.2 until 9.5 hours and the eluent contained 200.00 ppm of hardness. After 9.5 hours, the hardness level in the eluent showed a gradual increase and reached and remained at the same level as the influent's hardness (600 ppm) after 28 hours.

In Figure 4.2, the C/C_0 on the Y-axis is the ratio between the hardness concentrations in eluent to the initial hardness concentration in the incoming water to the column. As per the rationale developed above based on CKDu prevalence and the hardness values of waters in CKDu prevalent areas, the hardness level in the water needs to be lowered up

to 200.00 ppm. Thus, based on the breakthrough curve, it was observed that the constructed column with the cation exchange resin could be continuously used for 16 hours removal of hardness to levels <200 ppm. Further, according to the manufacturer's guidelines, the column was backwashed with a 10% NaCl solution to use it again.

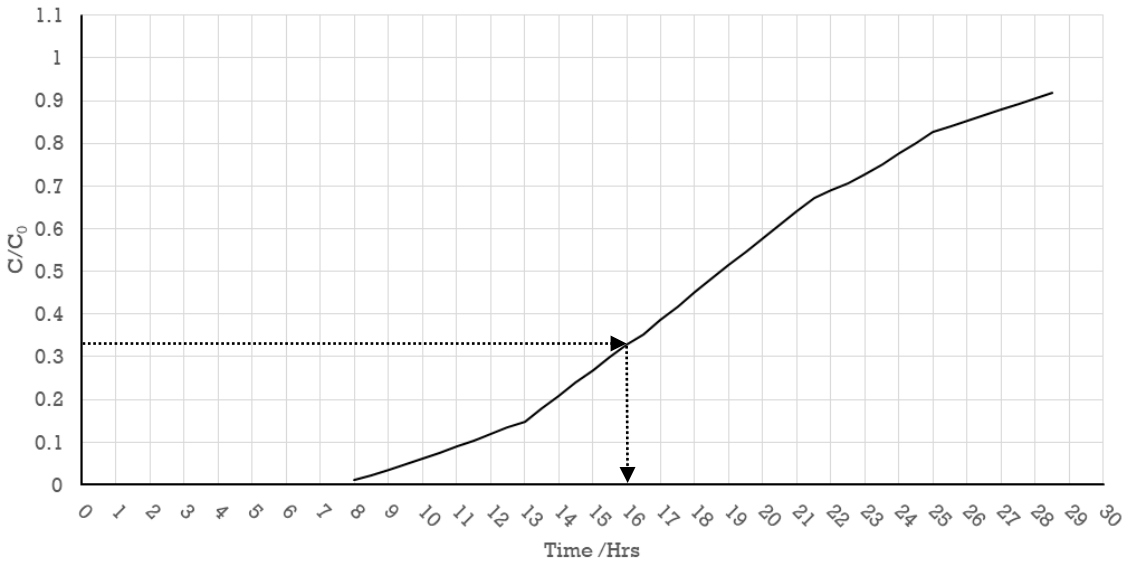

Figure 4.2 Breakthrough curve for hardness removal with the cation exchange column

4.2.2 The interactions of hardness and Fluoride inside the Cation Exchange Column in relation with Ion pair formation between Magnesium and Fluoride

Throughout the column experiment, the fluoride level in the eluent was similar to that of the influent because there was no way to remove fluoride from the divalent cation exchange column, due to the resin was exclusively designed for divalent cation removal. Moreover, when the synthetic water was prepared to provide conditions, that are similar to the water present in CKDu prevalent areas, the final fluoride level of the synthetic water with hardness + fluoride (2.6 ppm) was less than the initially added fluoride amount (3.0 ppm). This implies, that a certain amount of fluoride is not present as

fluoride ions alone; they may have transformed their chemical nature to some other ions. The possible ion pairs that could form in the mixture of hardness + fluoride would be CaF_2 or MgF^+ or both.

Since the fluoride levels in the eluent were unchanged during the experiment period of 29 hours, it was assumed that the formation of the MgF^+ ion pair was negligible. According to Shigel and Shigel (2019) in a mixture of Fluoride and Hardness solution (10 M = 1899 ppm), only 20% of fluoride will be converted to MgF^+. In the present study, the Fluoride concentration used was far lesser than 1899 ppm. Therefore, even if the MgF^+ ion pair may be formed, it may be present in trace levels and such levels may not be detectable due to the limitation of the methods. (The minimum detectable limit of IC is 0.01ppm)

Further, according to Dharma-Wardena (2017), at a closer range (The distance has not been given by the author) the Mg^{2+} and F^- will break apart under the electric fields of the ionic centers too (Dharma-wardena, 2017). On the other hand, the K_{sp} value for CaF_2 is $3.9*10^{-11,}$ and, it is always less than the K_C value of the synthetic solution (2.3×10^{-6}) for CaF_2. Thus, the formation of CaF_2 in waters in CKDu prevalent areas can be expected. The eluent was filtered using a filter paper (Whatman No 235) and any white-colored precipitate for CaF_2 or change in the filter paperweight was not observed. Since advanced techniques such as Potentiometry, which is the method applied to measure the existence of ion pairs, were not available, and therefore, the formation of ion pairs in the solution could not be confirmed.

The hardness of water is relatively higher in CKDu prevalent areas than CKDu non-prevalent areas. The simultaneous presence of Mg^{2+} and (Dharma-wardena, 2017) in water has been suggested as a cause for their modified toxicity effects compared to when these ions are present in potable groundwater alone. Moreover, the formation of ion-pairs is proposed as the reason for observed toxicities (Dharma-wardena, 2017). Ion pair formation between the cation and anion occurs if the Gibbs free energy of the hydrated ion pair is less than the summation of the respective individual hydration free energies of

the cation and anion. As explained by Dharma-wardena (2017), the estimated Gibbs free energies (kJ/mole) (ΔG^0 per mole) for Mg and F for MgF^+ Ion pair formation is -545 kJ/mole and it is a spontaneous reaction. The nephrotoxic effects of MgF^+ is described in detail by Dharma-wardena (2017).

Therefore, the hardness and Fluoride levels need to be reduced to levels that are not nephrotoxic to lessen the effect of ion pairing. As a baseline, it would be noteworthy to reduce the hardness and fluoride concentrations in drinking water in CKDu prevalent areas similar to that of hardness and fluoride concentrations present in CKDu non-prevalent areas. The need for developing a cost-effective, efficient defluoridation material is a solution that is of the utmost importance.

As the next stage of the present study, the eluent of the ion-exchange column was used and treated using an adsorbent (Functionalized Modified Fly Ash(FMFA)opt) for the removal of fluoride to overcome the postulated hypothesis of the formation of MgF^+, one of the suspected causal agent for CKDu as attributed above attempting to remove fluoride ions in the solution similar to the fluoride levels in CKDu non-prevalent areas(0.47 ppm or below) assuming there would not be synergy between hardness and fluoride once their concentrations are brought down to their concentrations in CKDu noon prevalent areas.

4.3 Characterization of defluoridation materials

The synthesized MFA,$(FMFA)_{opt}$, FA$(FMFA)_{opt}$ were characterized using SEM, EDX, FTIR, and XRD to identify the morphology, elemental composition, functional groups, and the structural changes during the modification process and after the adsorption of fluoride to understand the mechanisms for functionalization and defluoridation

4.3.1 XRD analysis of MFA, $(FMFA)_{opt}$ and FA$(FMFA)_{opt}$

The XRD spectra for MFA in Figure 4.3 represents peaks at 12.3 (110), 17.6 (020), 21.6 (311), 28.0 (131), 30.9 (022), 33.2 (112), 51.3 (804), and 62.8 (916). The same observations have been reported by Querol et al. (2002) in XRD analysis for P zeolite.

Further characterization of MFA sing FTIR analysis and SEM/EDX analysis will help to confirm the exact structure of the MFA.

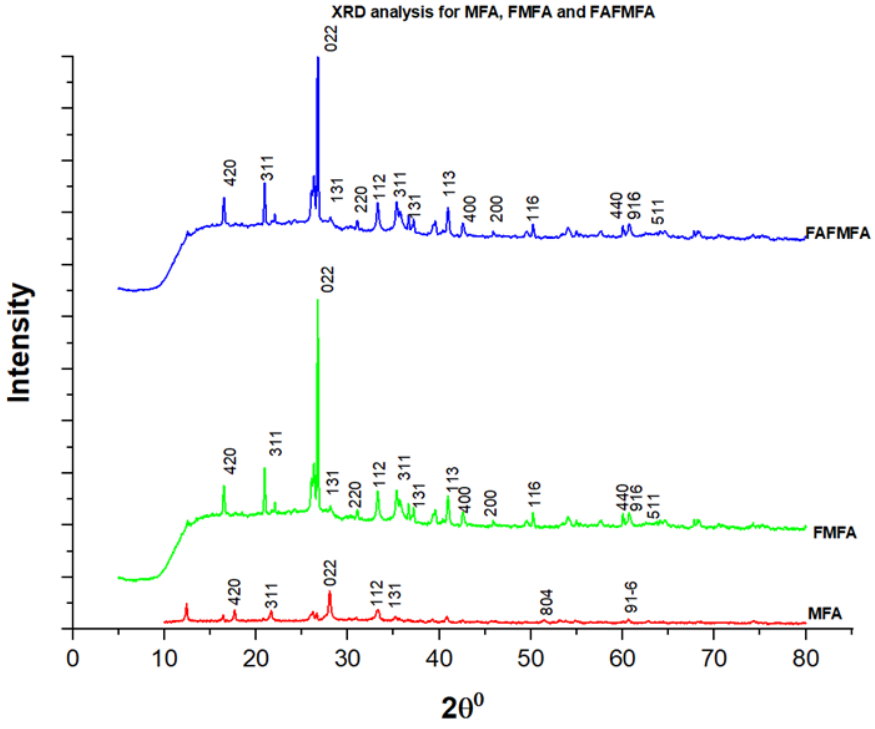

Figure 4.3 XRD analysis of MFA, FMFA, and FAFMFA

The peak pattern of the XRD spectra of $(FMFA)_{opt}$ are attributed more similarities with the XRD spectra of the MFA. Therefore, both MFA and $(FMFA)_{opt}$ should have more similar crystalline structures such as P–zeolite. Slight changes in the intensities of the diffraction peak were observed due to the functionalization. The addition of Fe into modified fly ash might lead to an increase or decrease of the intensities diffraction patterns of the same peaks without changing the crystallinity of MFA. The new planes at (4,40), (311), (200) representing Fe and its oxides in $(FMFA)_{opt}$ confirms the impregnation of Fe into MFA. As seen in XRD Fe is mainly bound to MFA as Fe_2O_3 (JCPDS card no. 18-0639).

The average crystalline size of the MFA was calculated from the XRD spectrum using Scherrer Formula as given in Equation 7 (Chekli et al., 2016).

$$D = \frac{0.9\lambda}{\beta \cos\theta} \quad (7)$$

Where the average crystalline size is given by *D*, the wavelength of the X-ray radiation is given as λ, the full width of half maximum of a diffraction peak is given as β, and θ is the angle of diffraction. The average crystalline size obtained from XRD data was 31.8 nm, which confirms that synthesized MFA was within the nano-scale. The calculated average crystalline size for $(FMFA)_{opt}$ was 31.25 nm, thus the major fraction of (FMFA)opt was in nanoscale.

The number of diffraction peaks have not been changed in $FA(FMFA)_{opt}$, indicating that no crystalline transformation occurs during treatment. But some slight peak shifts indicate the chemical composition has changed due to the adsorption of fluoride on $(FMFA)_{opt}$. The decrease of the intensity might result due to a higher absorption coefficient of fluoride compounds for the X-ray radiation and the lowering of FMFA content in the samples due to the addition of fluoride (Yang et al., 2005).

4.3.2 ESEM and EDX analysis of FA, MFA, $(FMFA)_{opt}$ and $FA(FMFA)_{opt}$

The ESEM and EDX of image for raw FA are given in Figure 4.4 (ai & aii). Sphere-shaped structures and small flakes with no definitive shape are present on the surface of FA. EDX analysis of FA, illustrated the elemental composition and their respective percentages on the surface of FA such as oxygen (O) 59.4%, Aluminum (Al) 11.3%, Silicon (Si) 18.2%, Sodium (Na) 8.3%, Magnesium (Mg) 0.3%, Potassium (K) 0.5%, calcium (Ca) 0.6%, titanium (Ti) 0.4% and iron (Fe) 1.1%. Once FA is converted to MFA, the shape in the defined structures has become more compacted, elongated with a definitive shape similar to long prisms lying all over the surface of the MFA as shown in Figure 4.4 (b_i). When FA is modified into MFA, the impurities in FA have been removed. The Al content in MFA is higher compared to FA and it may be the reason for the changing of the morphology of MFA. According to the results obtained from EDX analysis of MFA given in Figure 4.4 (b_{ii}), the elemental composition of the surface comprises of O (59.3%), Na (8.3%), Al (11.3%), Si (18.2%), Fe (1.1%), K (0.5%), Ti

(0.4%), Mg (0.3%), and Ca (0.6%). The Si: Al atomic ratio of MFA is 1.6 and that is lesser than the Si: Al ratio of coal fly ash (1.96) (Nugteren et al., 2011). Si: Al ratio of natural zeolite has been reported as 4.34 (Yuni et al., 2015). Therefore, MFA is an ideal adsorbent which can use to modify with cation for defluoridation due to the presence of a negative charge on Al on the surface.

Once the MFA was functionalized with iron oxide, the surface of the $(FMFA)_{opt}$ changed and appeared as a mixture of the deformed prism-like structures. The flake-like sharp structures on the surface of $(FMFA)_{opt}$ are covering a sheath-like structure as given in Figure 4.4 (c_i). The elemental composition of EDX analysis of $(FMFA)_{opt}$ shows that the surface is composed with O (62.4%), Na (4.4%), Al (5.9%), Si (9.2%), Fe (15.8%), K (0.5%), Ti (0.3%), Mg (5.9%), and Ca (0.5%). The EDX analysis of Figure 4.4 (c_i) confirms the impregnation of Fe into MFA. The deformation of the prismlike structure of $(FMFA)_{opt}$ might be appeared due to the incorporation of different forms of Fe into MFA.

After adsorption of fluoride, the surface morphology of $FA(FMFA)_{opt}$ has become shape undefined cloud-like structures [Figure 4.4 (d_i)]. The surface morphological changes of $FA(FMFA)_{opt}$ may be attributed due to the formation of different chemical structures after the adsorption of fluoride.

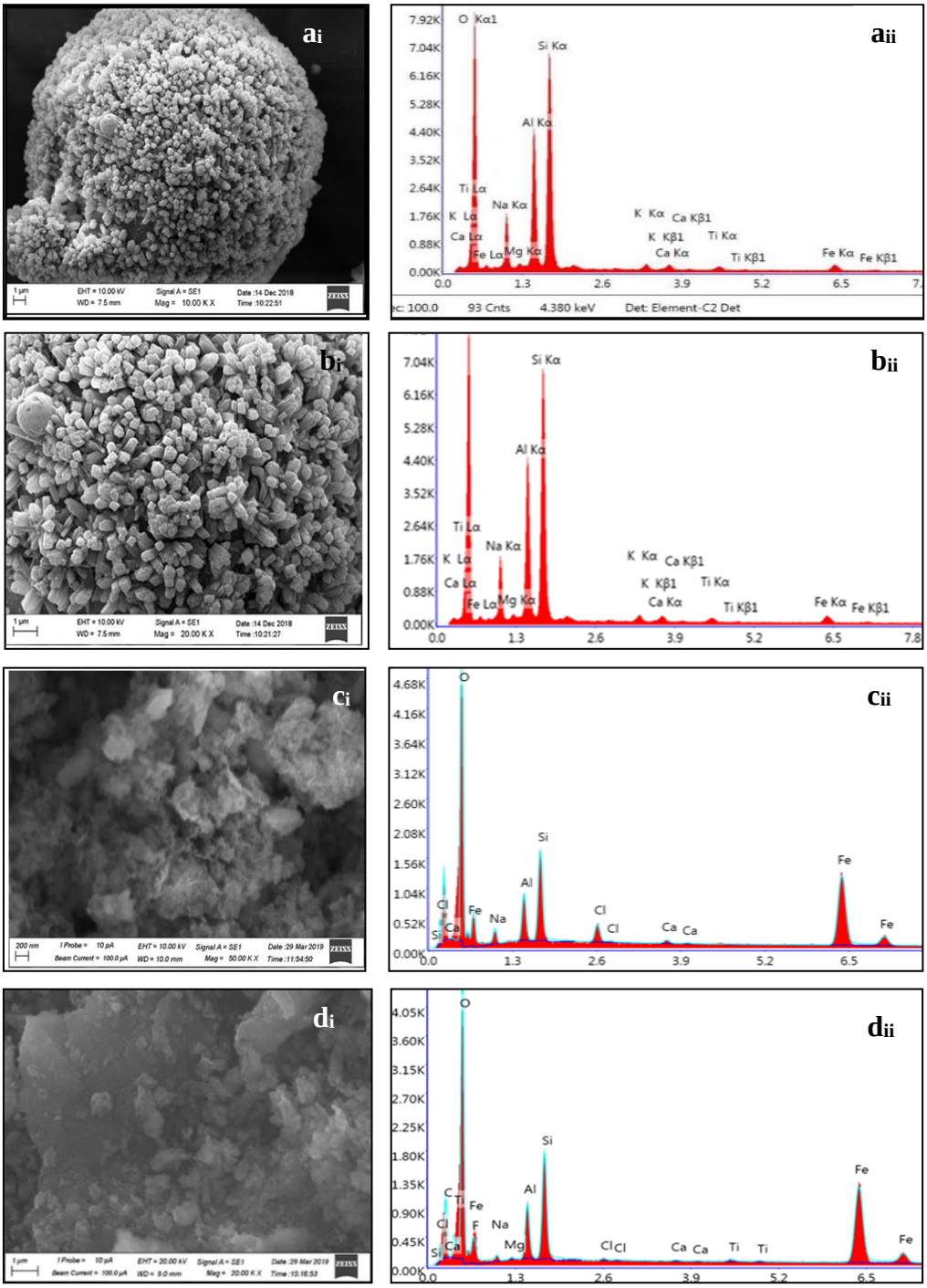

Figure 4.4 ESEM/EDX analysis analysis of (a_i & a_{ii}) FA, (b_i & b_{ii}) MFA, (c_i & c_{ii}) $(FMFA)_{opt}$ and (d_i & d_{ii}) $FA(FMFA)_{opt}$

The incorporation of fluoride on FA(FMFA)$_{opt}$ is confirmed with the EDX analysis as shown in Figure 4.4 (d_{ii}). The elemental composition of FA(FMFA)$_{opt}$ has shown as O (52.5%), Na (11.7%), Mg (1.3%), Al (6.2%), Ca (0.9%), Si (7.3%), Ti (0.2%), Fe (19.1%), and F (0.6%).The elemental percentages of Na had been increased due to the release of Fe^{2+} and Fe^{3+} ions from negatively charged Al centers and OH^- groups during the defluoridation process to bind with fluoride. Thus, the remaining Na ions might have reached to vacant negative charges in (FMFA)$_{opt}$. There is an increase in the elemental composition of Ca and Mg. Ca^{2+} ions and Mg^{2+} ions from the synthetic solution used for defluoridation might have been bound on adsorbent may be the reason of increasing Ca and Mg composition in FA(FMFA)$_{opt}$.

4.3.3 FTIR analysis for MFA, (FMFA)$_{opt}$ and FA(FMFA)$_{opt}$

The functional groups and bond patterns play a crucial role in adsorption. Before a suitable adsorbent is selected for defluoridation, understanding of the chemical reaction by which the defluridation occurs is of utmost importance. Every specific chemical bond of FTIR has its own specific energy absorption band and therefore, structural and bond information of a compound can be used to explain its chemical reactivity. The same principle can be applied to study the incorporation of (FMFA)opt to decide whether the adsorbent is potential enough to adsorb the desired adsorbate based on the functional groups present in the spectrum. The FTIR spectra for MFA (FMFA)$_{opt}$ and FA(FMFA)$_{opt}$ are given in Figure 4.5.

The peaks of MFA representing at 3417.07 cm^{-1}, 1635.83 cm^{-1}, 1447.83 cm^{-1}, 992.31 cm^{-1}, are attributed to O-H stretching vibration, bending vibration of water, O-H stretching vibration, Si-O sym-stretching, respectively. The three peaks at 595.17cm^{-1}, 576.00 cm^{-1}, 560.33 cm^{-1} are attributed to Al-O stretching. The FTIR spectrum of MFA is very similar to the FTIR spectrum for P zeolite studied by Zholobenko et al., (1998). Therefore, the surface modification of MFA with multivalent cations like Fe^{3+}, Fe^{2+} is ideal to generate a positive charge on the negatively charged MFA surface to enhance its surface properties for defluoridation.

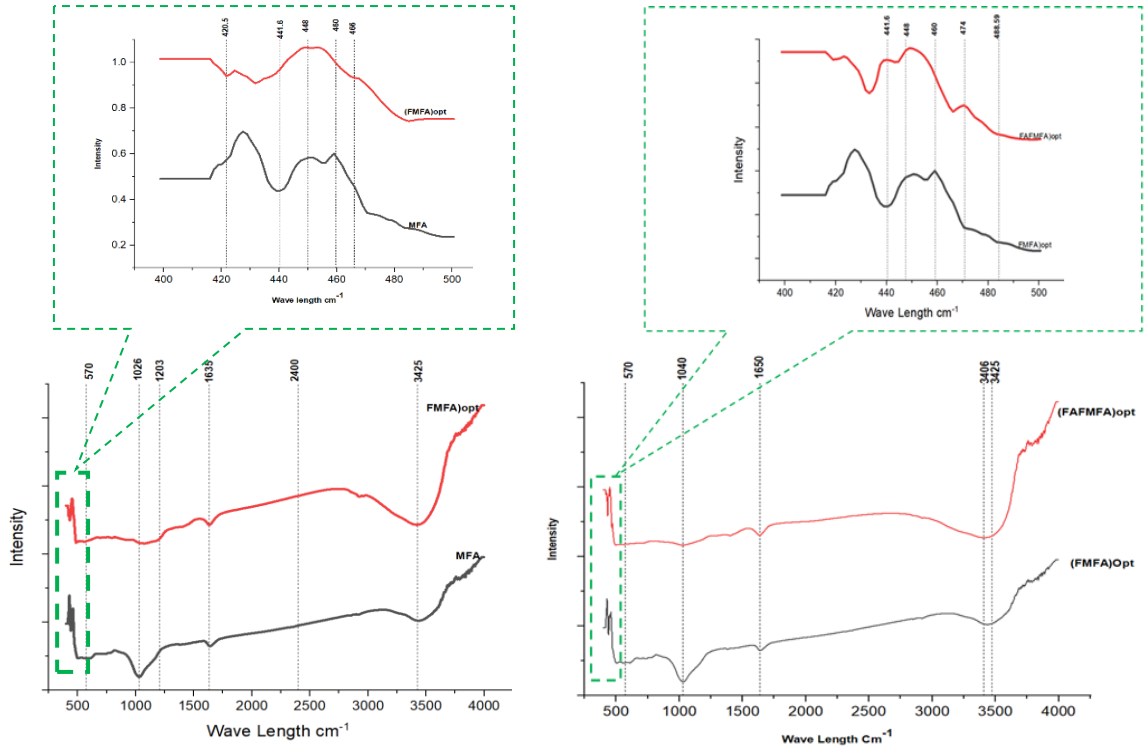

Figure 4.5 FTIR analysis of MFA, (FMFA)opt and FA(FMFA)$_{opt}$

The spectra produced by (FMFA)$_{opt}$ has a more similar pattern with the MFA. Therefore, there would not be any significant alteration of functional groups due to the modification of MFA with Fe. Once MFA is modified with Fe, the intensity of FTIR peaks of (FMFA)$_{opt}$ have been increased, decreased and some peaks have moved, and new peaks have appeared. The incorporation of Fe into MFA is shown in the 400 cm^{-1} – 600 cm^{-1} regions of the FTIR spectrum of (FMFA)$_{opt}$. The sharp variations of peaks due to the incorporation of Fe into MFA can be observed in the magnified image representing FTIR peaks of 400 cm^{-1} – 500 cm^{-1}. The peak intensities and its corresponding functional groups that appeared in FTIR spectra are summarized in *Table 4.1*.

Table 4.1 Different function groups present on MFA, $(FMFA)_{opt}$ and $FA(FMFA)_{opt}$

$(FMFA)_{opt}$		**$FA(FMFA)_{opt}$**	
Wavelength (cm^{-1})	**Corresponding Functional group**	**Wavelength (cm^{-1})**	**Corresponding Functional group**
468	O-Si-O Bending Vibration	420.5	FeO bond in FeOH Oxide
555	Si-O-Si Bending Vibration	441.6	F on Ze
448	Ze FeO	448.0	Ze FeO
455	Ze	455.0	Ze
420.5	FeO bond in FeOH Oxide	460.0	Fe2O3
400-450	Opening of Zeolite Pores	462.0	Pure Zeolite
441.6	F on Ze	468.0	O-Si-O Bending Vibration
462	FeO-Fe-AlO	474.7	Fe-F Bond
460	Fe2O3	474.7	Fe-F Bond
546	Al-O/Si-O bond	488.6	CaF Bending
570	FeO Vibration	546.0	Al-O/Si-O bond
462	Pure Zeolite	555.0	Si-O-Si Bending Vibration
1203	SiO Stretching	570.0	FeO Vibration
1635	Bending mode of surface adsorbed water in bare Iron oxide	1203.0	SiO Stretching
3425	Surface Hydroxyl	1635.0	Bending mode of surface adsorbed water in bare Ion oxide
		3406.0	FeOCaF Bond

Source: (Mozgawa et al., (2011); Zholobenko et al., (1998); Peña and Rondón, (2013), Jayarathne et al., (2015), Sudasinghe etal., (2019)

The peaks at 450 - 600 cm^{-1} show the presence of different bonding forms FeO on the surface of the MFA and FeO vibrations. The peak produced by FeO has a very large intensity and the resulting curve is very sharp. The decrease in absorption in wavenumbers between 450-400 cm^{-1} confirms the presence of Van der Waals forces between zeolites and FeO. When Fe_2O_3 is combined with zeolite via Fe-O-Si or Fe-O-Al, the presence of Fe-O-binding force is bounded by a surface bond on the zeolite structure causes the energy absorption in FTIR (Parraki et al., 2004). A decrease in absorption has occurred between the wavenumbers of 500-420 cm^{-1} due to Fe-O SiO/ AlO bending vibration. It decreases the bonding between Zeolite and Zeolite-FeO. The size of the area produced in Zeolite-FeO is smaller than that of Zeolite, due to the reduced bending between SiO/AlO. A stretching vibration involving a tetrahedral atom can be seen in the 650-820 cm^{-1} region (Suhartana et al., 2018).

Another opinion of the region of the wavenumbers between 400 - 450 cm^{-1} indicates the opening of zeolite pores (Araujo et al., 1999) and it might be favorable for Fe ions to move into the inside of the porous MFA structure for a better modification. Compared to MFA, a significant increase in peak intensities in this region can be observed.

After the adsorption of , the peak intensity responsible for functional groups has been changed as shown in Figure 4.6. New peaks are shown in $FA(FMFA)_{opt}$ spectra in 474.7 cm^{-1},488.6 cm^{-1}, 1383 cm^{-1} 3205 cm^{-1} and 3406.00cm^{-1} corresponding for Fe-F bond, Ca-F bond, Fe-F bond, Fe–O–Ca–F, and Fe–F respectively (Yuan et al., 2008; Patnaik et al., 2016; Liu et al., 2018; Jayarathna et al., 2015; Galván-Ruiz et al., 2009; Sudasinghe et al.,2019; Tahvildari et al., 2012).

The broad peak visible in between 3000–4000 cm^{-1} in $(FMFA)_{opt}$ responsible for surface-bound OH^- ions in $(FMFA)_{opt}$ has been shifted right and a new peak had been created 3420 cm^{-1} in $FA(FMFA)_{opt}$ after the adsorption of fluoride (Raul et al., 2012; Jayarathna et al., 2015). This shifting of OH- group may be due to the exchange of the OH^- group with fluoride and hydroxyl groups in $(FMFA)_{opt}$ may become free from hydrogen bonding with $(FMFA)_{opt}$ and therefore it is evident that the OH^- groups on

$(FMFA)_{opt}$ significantly contributing for the defluoridation process (Jayarathna et al., 2015). There is an H balancing cation on the zeolite skeleton. When the presence of an H-balancing cation on MFA, it can be modified with Fe_2O_3 to form zeolite-Fe (Oliveira et al., 2016).

4.4 Selection of best combination of MFA: Fe ratio to remove fluoride in the presence of hardness

The defluoridation capacity of different weight combinations of MFA: Fe was studied to select the optimum ratio of Fe: MFA for the defluoridation. The obtained results of defluoridation for each combination are given in *Table 4.2*.

Table 4.2 The defluoridation capacity of different combinations of MFA: Fe

MFA: Fe Weight ratio	Initial Concentration (mg/L)	Final Concentration (mg/L)	Removal Efficiency (%)
2:0(1)	2.3	1.62	29
1:1(2)	2.3	0.38	83
1:2(3)	2.3	0.63	72
2:1(4)	2.3	0.75	67
3:1(5)	2.3	0.77	66

The maximum defluoridation efficiency was observed when the Fe: MFA ratio was 1:1 where the lowest defluoridation efficiency was given when the MFA: Fe ratio was 2:0. Therefore, the ratio 1:1 MFA to Fe combination was selected to conduct further the defluoridation experiments.

4.4.1 Mechanisms for impregnation of Fe on MFA surface and the defluoridation with$(FMFA)_{opt}$

MFA has a net negative charge on its Al center. Therefore, when it is treated with Fe_{3+}, Fe^{3+} goes and binds with the negatively charged Al center and then MFA gets a net positive charge (Danabas et al., 1992). Moreover, Fe atoms can replace protons from acidic MFA and Fe ions can bind with OH groups in MFA. The reaction is exothermic

(1384 Kj/mol) and favorable. Further, the ionic radius of Fe^{2+} and Fe^{3+} is lesser than the pore size of MFA. (The ionic radius of Fe^{2+} Fe^{3+} and pore diameter of MFA are 63 pm,77 pm, and 4500 pm respectively) (Sanchez, 2017; Moribe, 2010). Thus, Fe ions can easily go and bind with negative charges in MFA. During the calcination process, Fe^{3+} is oxidized and its oxidized forms are present in $(FMFA)_{opt}$ and when defluoridation occurs in aqueous media, the oxidized forms of Fe are converted to its hydroxides. During the modification, Iron oxide clusters in the zeolite pores could also be formed, especially at high iron loading (Gurgul et al., 2013). However, due to high electronegativity in fluoride ions and the similarity of the ionic radius of fluoride ions and hydroxyl ions, fluoride ions in incoming water substitutes OH^- ions in MFA and defluoridation occurs.

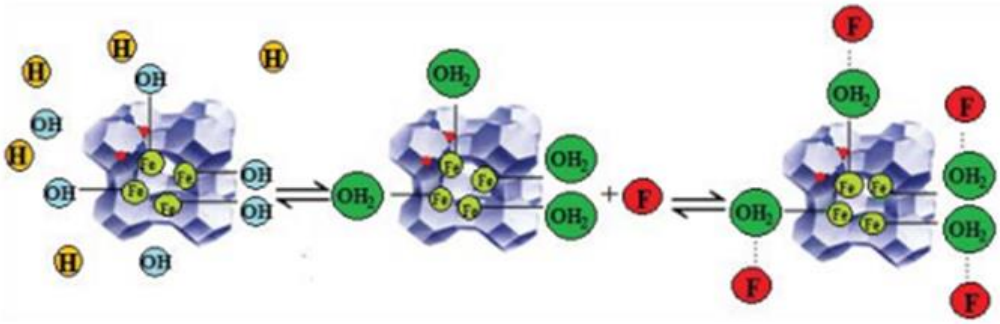

Figure 4.6 Schematic illustration of fluoride adsorption by FMFA via complex formations (Abaei et al., 2017)

The behavior of $(FMFA)_{opt}$ in aqueous medium discussed by (González et al. (2001) and Onyango et al. (2004) are given in Equation 8 and 9.

$$ZeO\text{-}FeOH + H^+ \rightleftharpoons ZeO\text{-}FeOH^{2+} \quad (8)$$

$$ZeO\text{-}FeOH \rightleftharpoons H^+ + ZeO\text{-}FeO^- \quad (9)$$

The adsorption of fluoride ions on $(FMFA)_{opt}$ by ion exchange process or via Vanderwal interactions are given in Equation 10-12 (Abaei et al., 2017):

$$ZeO\text{-}FeOH + \rightleftharpoons ZeO\text{-}FeF + OH^- \quad (10)$$

$$ZeO\text{-}FeOH^+ + \rightleftharpoons ZeO\text{-}FeF + H_2O \quad (11)$$

Or undergo non-specific columbic interaction through reaction

$$\text{Zeo-FeOH}^{+} + 2 \rightleftharpoons \text{Zeo-FeOH} + 2\text{F} \qquad (12)$$

Based on the experimental results given in *Table 4.2*, the lowest defluoridation was observed when the MFA: Fe weight combination was 2:0. When MFA is applied for defluoridation, only the exchange of with hydroxyl groups in the MFA structure may contribute to defluoridation. Moreover, Ca and Mg ions in the synthesized solution also may go and bind with negatively charged Al centers in MFA they may block the mobility of fluoride ions.

Maximum defluoridation was observed when the MFA: Fe ration is 1:1. The stoichiometry between MFA: Fe is 1:1, the ideal concentrations of each ion are present in the solution and fluoride ions may go and binds with positively charged Fe ions in the porous MFA structure.

When MFA: Fe ratio is lower, as less amount of Fe is present and there may be vacant negative charges. Therefore, there will be a repulsion between negatively charged aluminum centers and fluoride ions. This will hinder the binding of fluoride on active sites too. Thus, may repel negatively charged fluoride ions and defluorination efficiency is reduced. Moreover, due to the availability of negatively charged surfaces in FMFA structure, Ca^{2+} and Mg^{2+} ions may come and bind, and they may block the mobility of fluoride ions towards positively charged cationic canters. Base on the experimental results when the fly ash content is higher, the defluoridation ability is lessened.

When the MFA: Fe ratio is higher, iron can be deposited on the surface of MFA. During the calcination process, the deposited Fe is converted to Fe_2O_3. The deposition of iron blocks the pores of MFA, thus the route for the fluoride ions to transfer into the inside of the porous MFA structure can be blocked and the defluoridation efficiency can be retarded (Gurgul et al., 2013).

4.5 Batch adsorption studies of $(FMFA)_{opt}$ for the removal of fluoride

4.5.1 Effects of adsorbent dosage

The amount of adsorbent dosage plays a vital role in the determination of fluoride adsorption capacity of $(FMFA)_{opt}$ in the presence of hardness. The effect of $(FMFA)_{opt}$ dosage on the defluoridation were ascertained with $(FMFA)_{opt}$ loading of 0.05 – 1.70 g, when the initial fluoride concentration 2.1 mg/L and hardness concentration 200.0 mg/L, contact time 24 hours, initial pH 5.5 and stirring speed 100 rpm..

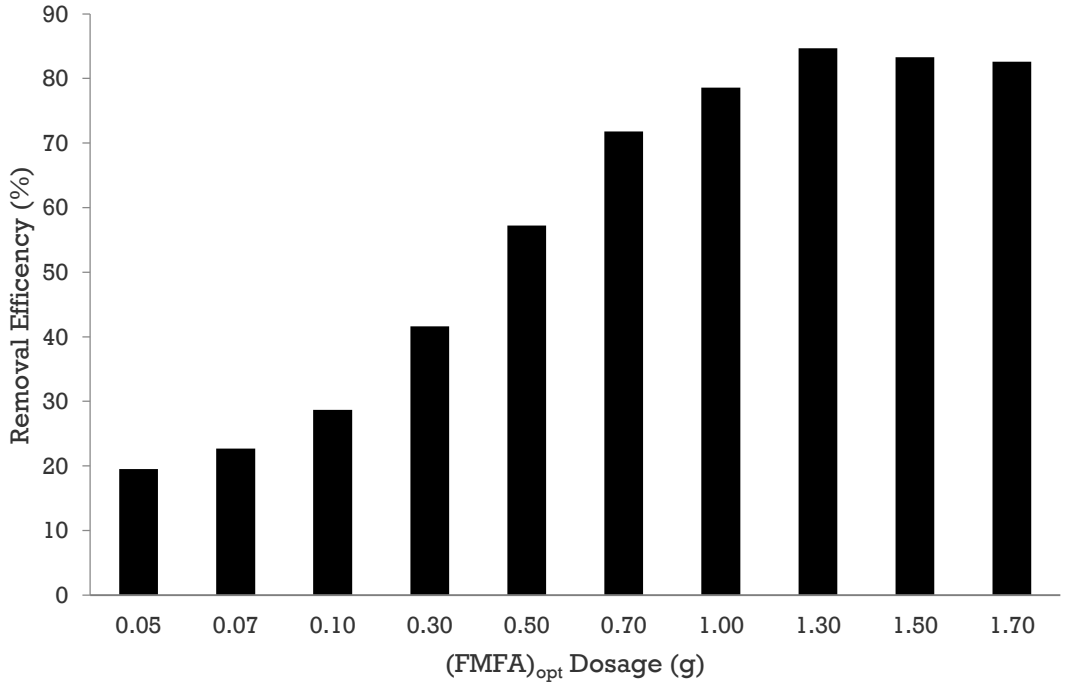

Figure 4.7 *Bar chart for optimum dosage selection for defluoridation using* $(FMFA)_{opt}$

The results show (Figure 4.7) that removal efficiency was sharply increased from 19.5% to 78.6% and later the system has reached the equilibrium after 1.0 g. When the adsorbent dosage is increased ion particle can be agglomerated due to its paramagnetic properties thus the number of adsorption sites may be limited (Knez et al., 2001 and Wang et al, 2009). The maximum removal percentage of $(FMFA)_{opt}$ was shown at the

dosage of 1.3 g. the 1.3 g of $(FMFA)_{opt}$ was used to determine the effects of contact time and solution pH for defluoridation

4.5.2 Effects of contact time

The effects of contact time in the removal of fluoride were determined within the contact time 0.5 – 60 minutes keeping initial fluoride concentration 2.1 mg/L and hardness concentration 200.0 ppm, $(FMFA)_{opt}$ dosage 1.3 g, initial at pH 5.5, and stirring speed at 100 rpm. When the contact time was increased, the removal efficiency of $(FMFA)_{opt}$ was increased from 2.5% to 84.2%, and the final concentration of fluoride was decreased (2.09 to 0.34 ppm) (Figure 4.8). A large amount of fluoride was adsorbed until the 30.0 minutes and after 30.0 minutes the system was reached to the equilibrium at about 40.0 minutes. The 40 minutes can be considered as optimum contact time which needs to treat for 100.00 mL of drinking water containing 200.00 mg/L hardness and 2.10 mg/L of fluoride.

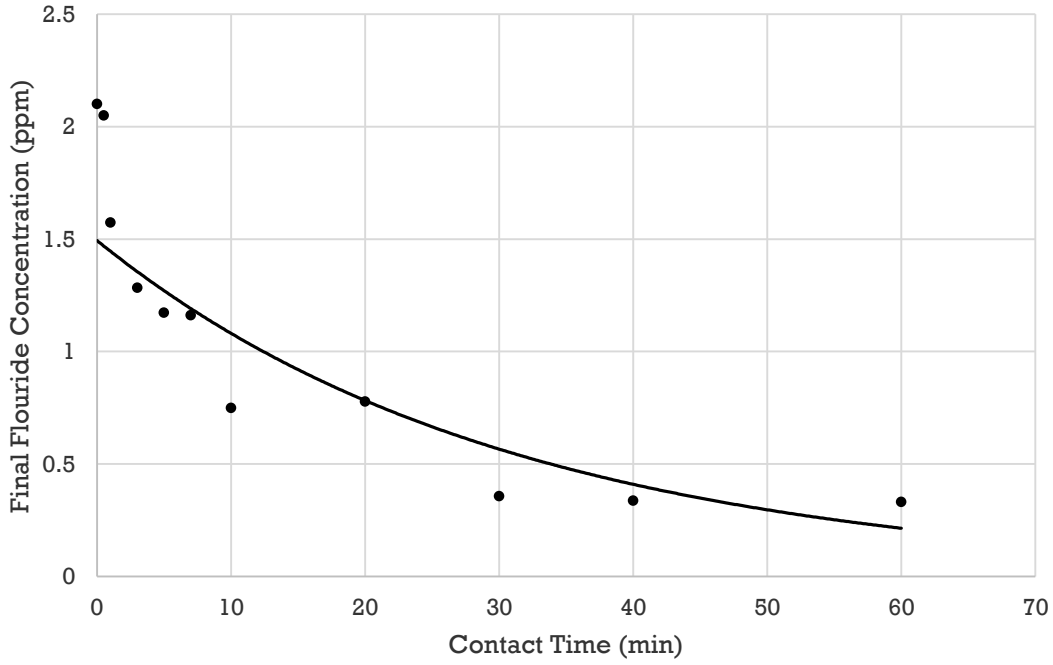

Figure 4.8 Scatter plot for the selection of optimum contact time for defluoridation

Based on Figure 4.8, initially, the defluoridation amount is less and it is gradually increased until 0 - 40 minutes of contact time. After 40 minutes of contact time, the fluoride removal rate seems to be low from 40 - 60 minutes. Initially, when the contact time is little, there is no enough time to contact all the adsorbate with the adsorbent and therefore the defluoridation amount is less at early contact times. The reduction of the rate of removal of fluoride when the contact time is increased is may be due to the saturation of all adsorption sites with adsorbate.

4.5.3 Effects of pH in the solution

The pH of the solution is a deterministic parameter and influence considerably in the removal of fluoride in the solution. The effects of pH on the adsorption of fluoride in the solution were determined varying the pH 2–10 for the initial fluoride concentration at 2.1 ppm and hardness concentration 200.0 ppm, adsorbent dosage 1.3 g, contact time for 40 minutes and the stirring speed is 100 rpm. The removal efficiency of $(FMFA)_{opt}$ was gradually increased (69.5%–83.0%) until about pH 6 and decreased (83.0%–66.6%) gradually at pH 9. The large adsorption capacity of $(FMFA)_{opt}$ was observed at pH 6.

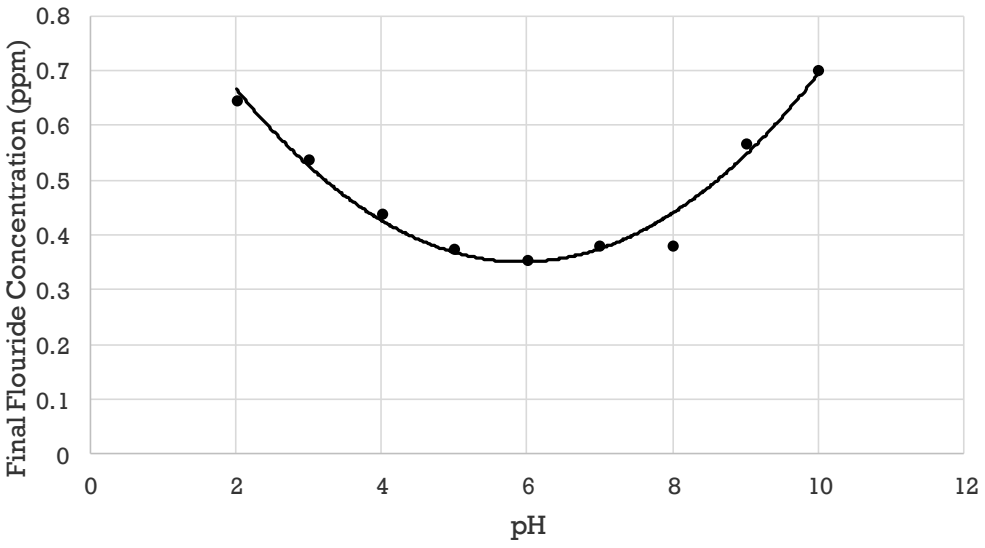

Figure 4.9 Defluoridation with $(FMFA)_{opt}$ at different pH levels

The adsorption of fluoride ions on the $(FMFA)_{opt}$ surface is controlled by the pH of the aqueous solution mainly due to the adsorption of fluoride ions on FMFA)opt by exchanging of fluoride ions with the OH^- ions in FMFA)opt during FTIR analysis.

The fluoride adsorption on Iron oxide has been modeled as a two-step ligand-exchange reaction as given in Equation 13–15 (Tripathy et al., 2006).

$$Fe\ (OH) + H^+ \rightarrow Fe(OH)^{2+} \quad (13)$$

$$Fe\ (OH)^{2+} + F^- \rightarrow FeF + H_2O \quad (14)$$

The net reaction is given as,

$$FeOH + H^+ + F^- \rightarrow FeF + H_2O \quad (15)$$

The material possessed about 83% removal efficiency at the initial fluoride concentration of 2.1 mg/L as illustrated in Figure 4.9. The higher adsorption at lower pH is due to the increase of H^+ on the adsorbent surface making the surface of the adsorbent positively charged. This results in an electrostatic attraction between positively charged adsorbent surface and fluoride ions. The decrease in removal efficiency at higher pH values can be due to the competition for the active sites by OH^- ions and the electrostatic repulsion of anionic fluoride by the negatively charged hydroxyl ions. pH zero point of charge is the pH value at which the sorbent exhibits zero net electrical charge on the surface when submerged into an electrolyte and positive charge on the surface is just below the pH ZPC. Fluoride removal above the point of zero charge pH value must have been by ion-exchange as OH^- ions would predominate over H_3O^+ ions (Isuagie et al., 2016). Therefore, the pH ZPC for the $(FMFA)_{opt}$ should be below 6.8 and the adsorbent ideally performs well in potable water.

The majority of adsorbents used for defluoridation work in a narrow-working pH range and the optimum performance has shown in the acidic pH range. However, the pH of natural groundwater in CKDu prevalent is in the range of 5.7 to 8.7 (Wanasinghe et al., 2018). The $(FMFA)_{opt}$ has given a maximum defluoridation at pH 6.00 and unlike other

most of defluoridizing agents, the synthesized material is well-matched with its optimum pH value with the normal pH of the groundwater present in CKDu prevalent areas.

4.6 Adsorption isotherms studies for $(FMFA)_{opt}$

Adsorption isotherms are applied in describing the binding mechanism of adsorbate on an adsorbent and helps to estimate the maximum amount of adsorbate adsorbed at equilibrium. Hence, the adsorption isotherm indicates the suitability of an adsorbent for the relevant application (Thembukar et al., 2016). The Freundlich and Langmuir isotherms are the most used models to investigate the adsorption behavior of adsorbent. The experimental data were fitted with Freundlich and Langmuir isotherms and the isotherm constants were calculated using the slope and intercept of the plotted data (Figure 4.10).

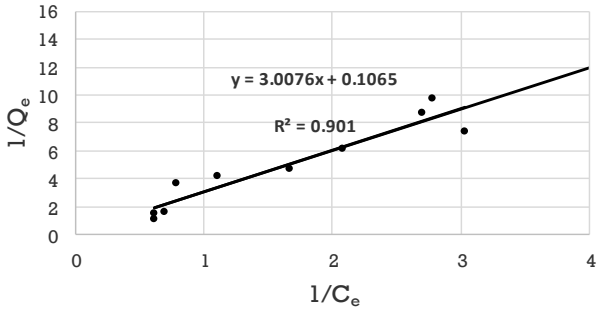

(a)

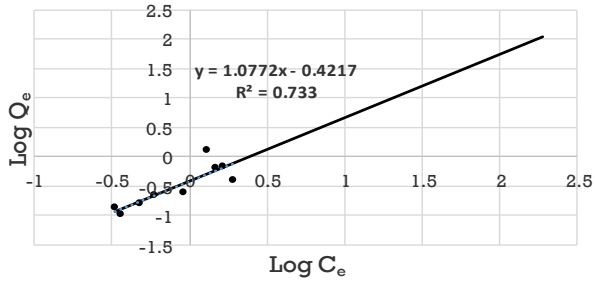

(b)

Figure 4.10 Adsorption isotherms (a) Langmuir isotherm and (b) Freundlich isotherm

The value of Langmuir constants such as Q_m, K_L and R_L of Langmuir model Figure 4.10(a) were calculated from the slope and intercept of the linear plot of 1/*Ce* versus 1/*Qe* as 10.0 mg/g, 0.81 L/mg and 1.23, respectively. The K_L value is above zero and therefore there a strong interaction between adsorbate molecules and the functional groups present in adsorbent can be expected. The separation factor for the Langmuir constant, (R_L), was calculated according to Equation 3. The value of R_L indicates that the experiment is "favorable" between 0 and 1 ($0 < R_L < 1$), "linear" $R_L = 1$ and "irreversible" $R_L = 0$. R_L value describe the shape of the isotherm and adsorption mechanisms. The obtained R_L value is 0.27, and it is in the range of "$0 > R_L > 1$" and therefore, the Langmuir adsorption is favorable for the defluoridation with $(FMFA)_{opt}$ The Langmuir model has a higher R^2 value (0.90) compared to the Freundlich model (R^2 – 0.73). The adsorption of fluoride data was well represented the Langmuire model, which indicates the adsorption mechanism follows the monolayer adsorption behavior and the adsorbent is having active sites with uniform energy on the surface of the adsorbent (Langumuir, 1916).

The plot for the Freundlich isotherm model is given in Figure 4.10(b). The R^2 value obtained when fitting the test values with the Freundlich isotherm Model was 0.733 and therefore, the adsorption of fluoride with $(FMFA)_{opt}$ does not strongly follow the Freundlich Isotherm.

4.7 Adsorption kinetics studies for $(FMFA)_{opt}$

The experimental data were fitted with kinetic models including, Pseudo first-order and pseudo-second-order models to determine the adsorption behaviour and the potential rate limiting mechanism. The Pseudo first order model explains that the adsorption rate is proportional to the first power of concentration, and the adsorption is said to be characterized by diffusion through a boundary (Srivastav et al., 2013). The pseudo-second-order model assumes that chemisorption may be the rate-controlling step in the adsorption processes (Ho and McKay, 1998).

The experimental data were fitted to the Pseudo first-order model by plotting log (Q_e-Q_t) Vs time (t) (Figure 4.11). The lower correlation coefficient (R^2- 0.32) was observed in Pseudo first-order model than Pseudo second-order model. Therefore, the rate of reaction is not proportional to the first power of the concentration of the reactant.

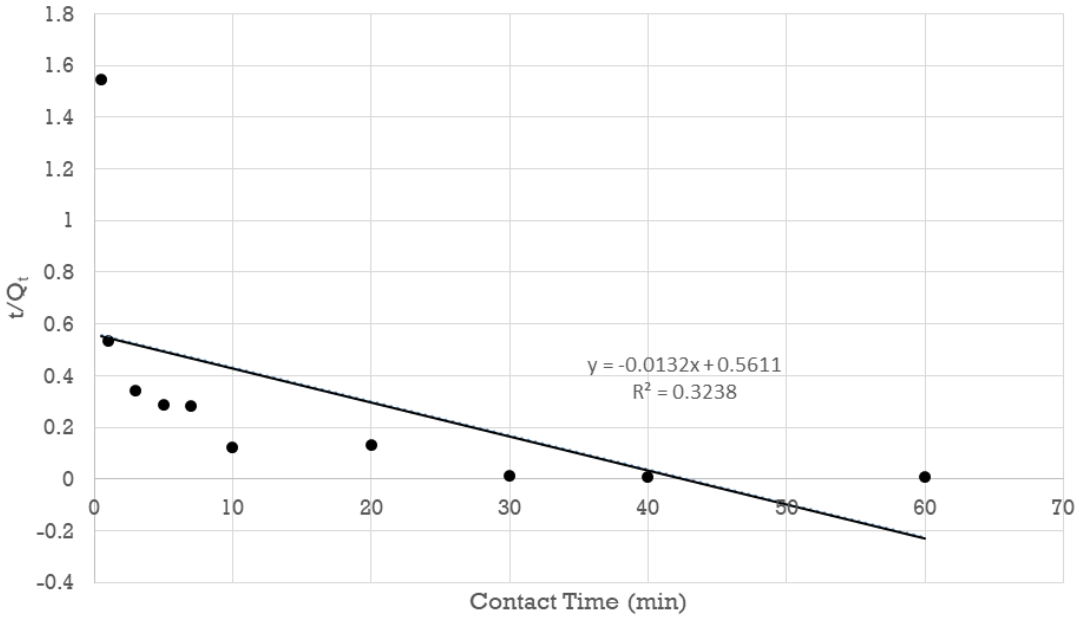

Figure 4.11 The pseudo-second-order kinetics model for the fluoride adsorption on to $(FMFA)_{opt}$

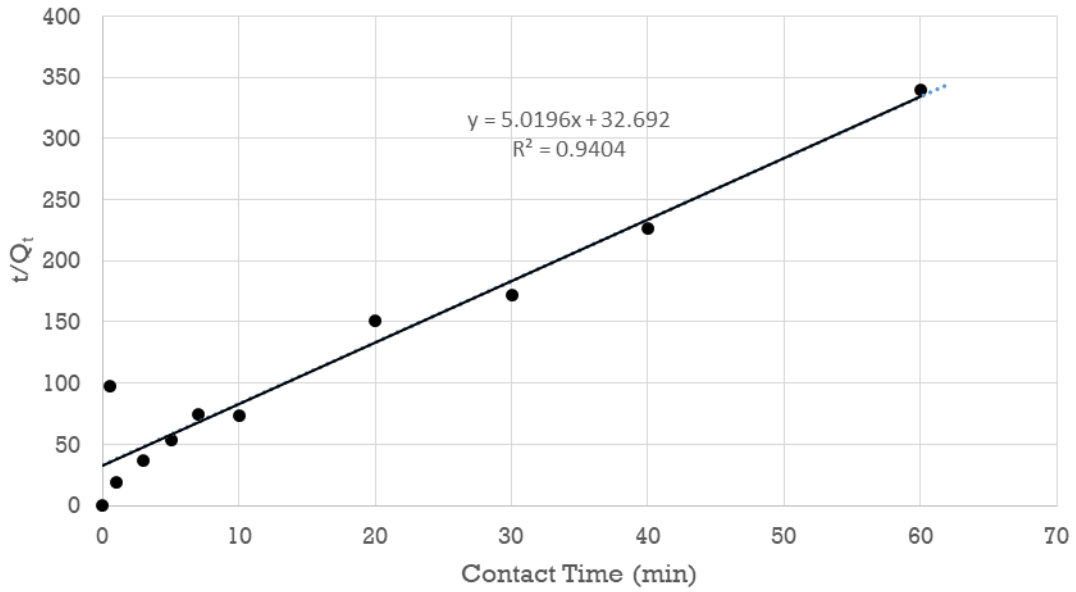

Figure 4.12 Pseudo Second-order kinetics for adsorption of Fluoride on $(FMFA)_{opt}$

The parameters of pseudo-second-order model were calculated using the slope and intercept of the plot given in Figure 4.12 between 1/*qe* Vs time (*t*). The R^2 value was calculated as 0.94 and the parameters of Q_e and K_2 were calculated as 27.64 mg/g and 4 x 10^{-5} mg^{-1} min^{-1}, respectively. The calculated experimental values Q_e approximately equal to the calculated Q_e value. The experimental data fit better with the pseudo-second-order model than pseudo-first-order model. Therefore, the chemical reactions are the rate-controlling step and the adsorption is done mainly through a chemical reaction (Ho and Mckay., 1999).

Gibbs free energy for the reaction can be calculated as below Equation 16.

$$\Delta G = -RT\ lnK \qquad (16)$$

K is the adsorption constant at equilibrium derived from Langmuir's equation at corresponding temperature, *R* is the gas constant (8.314 J/mol/K) and *T* is the absolute temperature (K). According to the calculation, if the value of ΔG is negative, the

adsorption reaction can conduct spontaneously, and the larger the value of ΔG, the higher the degree of spontaneous reaction (Wang et al., 2013).

The ΔG obtained for adsorption of fluoride on $(FMFA)_{opt}$ is -503.8. Therefore, the reaction is spontaneous.

4.8 Regeneration of the $(FAFMFA)_{opt}$

The regeneration studies were conducted to ascertain the regeneration potential of $(FMFA)_{opt}$ at different acidic, neutral, and alkaline media as described in materials and methods.

The $FA(FMFA)_{opt}$ was saturated completely using fluoride (2.1 mg/L) and hardness (200.0 mg/L) mixture and regenerated using different eluting agents such as EDTA (pH 7), HCl (pH 2), and NaOH (pH 12) (Figure 4.13 & Figure 4.14). The purpose of selecting regenerating regents at different pH ranges is to determine the regeneration potential of $(FMFA)_{opt}$ using different eluting agents at different pH values to select the most effective regeneration medium. The regeneration potential of FMFA with NaOH showed a higher defluoridation efficiency. This may be due to the exchange of fluoride ions with hydroxyl ions from the concentrated NaOH solution and again hydroxyl ion may have been contributed to remove fluoride. The fluoride removal efficiencies of the regenerated material after each regeneration cycle are given in Figure 4.13 & Figure 4.14. FMFA regenerated with NaOH was adsorbed fluoride in the solution to reach up to 0.47 mg/L or below during two regeneration cycles. From the study, it was observed that the FMFA has somewhat recycling and regeneration capacity and a cost calculation for regeneration should be conducted to check whether the refilling of the material or regeneration of the material is ideal when $(FMFA)_{opt}$ is applied in a commercial defluoridation system. When the number of regeneration cycles was increased it was observed that the final fluoride concentration in the solution was increased. The reduction of fluoride adsorption capacity may be due to saturation of adsorption sites due to ligand exchange, and the change of the chemical and physical properties on the surface of the adsorbent.

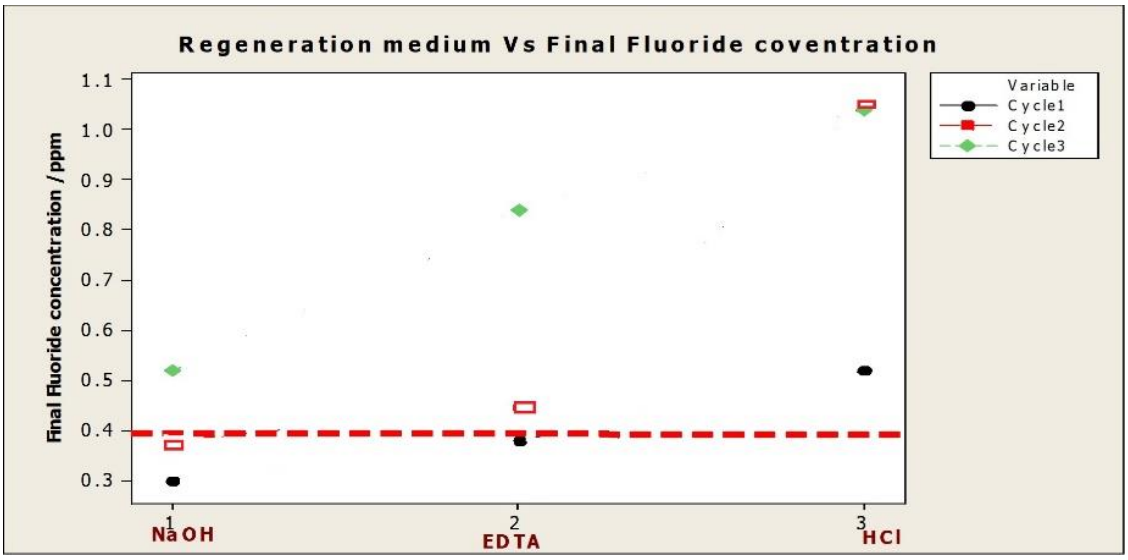

Figure 4.13 The final fluoride concentration obtained after using the regenerated material for each three regeneration cycles

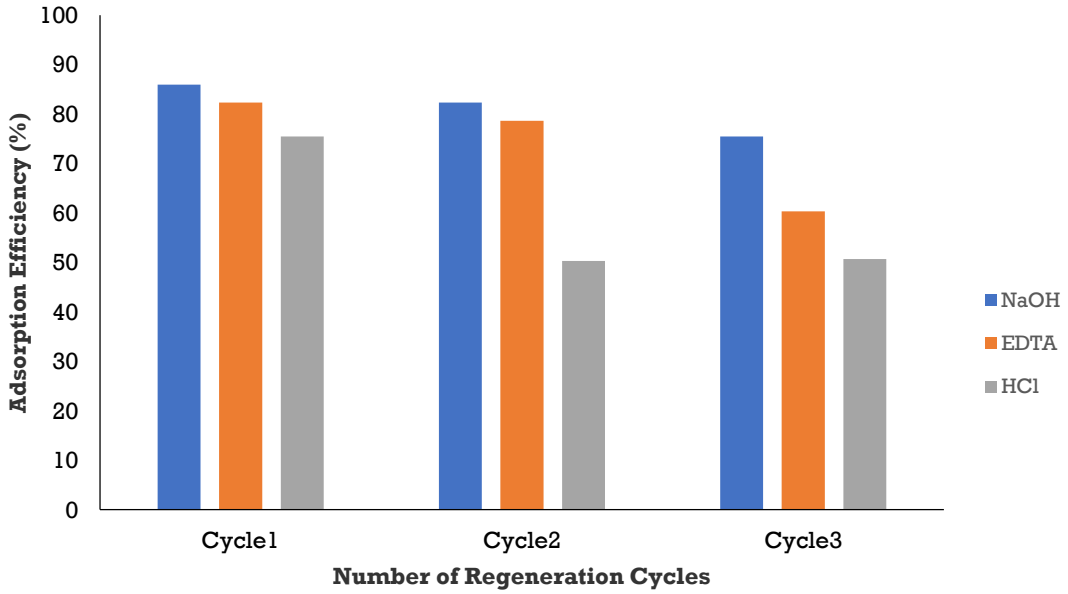

Figure 4.14 The fluoride adsorption efficiency of $(FMFA)_{opt}$ after each regeneration cycle

4.8.1 Characterization of regenerated materials

Surface morphology, elemental composition, and functional groups of the surface were ascertained using ESEM/EDX, and FTIR. The characterization of regenerated materials showed changes in the surface properties during the regeneration process. The changes in surface properties imply that the pH of the regeneration medium has a huge potential to change the surface morphology which affects the adsorption capacity of the $(FMFA)_{opt.}$

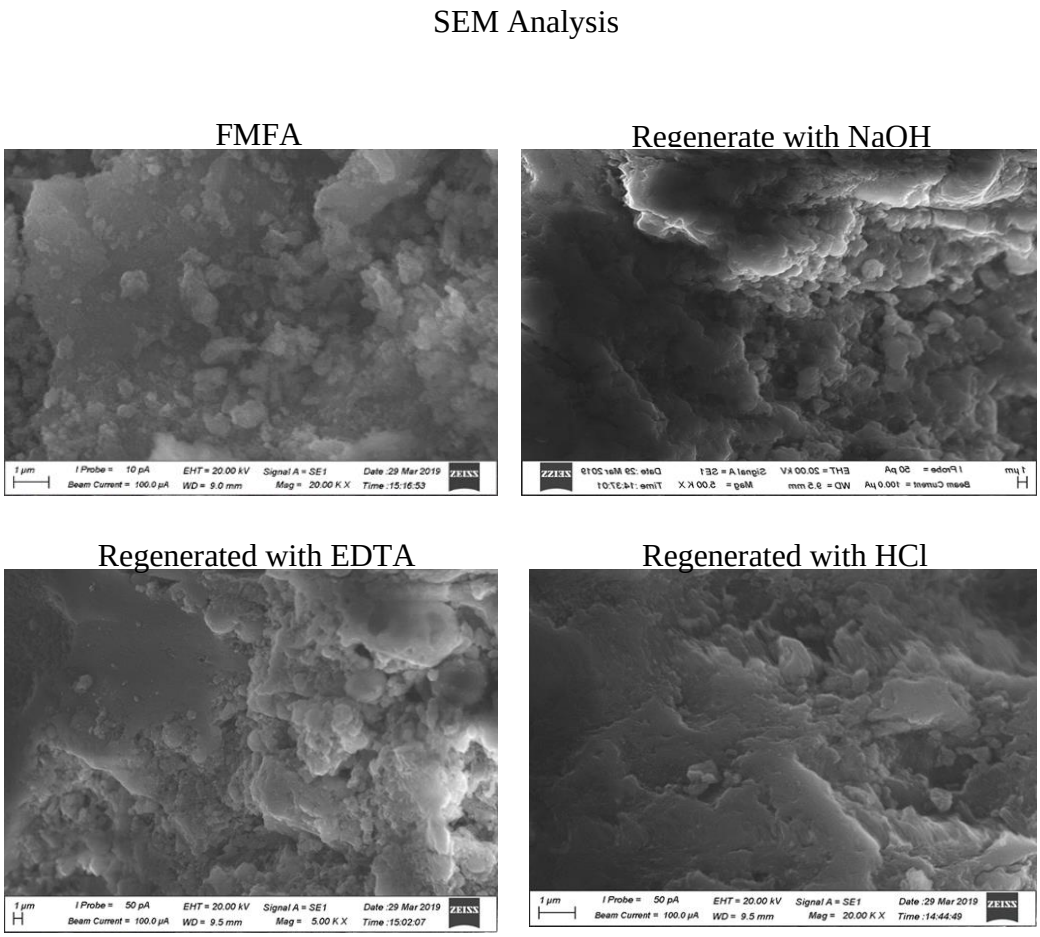

Figure 4.16 The Comparison of the SEM image of (FMFA)opt with SEM images of regenerated material after three regeneration cycles

ESEM images of the $(FMFA)_{opt}$ regenerated from NaOH, HCl and EDTA indicate the surface of the adsorbent have void surfaces with irregular, uneven flakes like structure which appears due to deformation and deterioration of the surface of the $(FMFA)_{opt}$ by eluting agents

FTIR Analysis

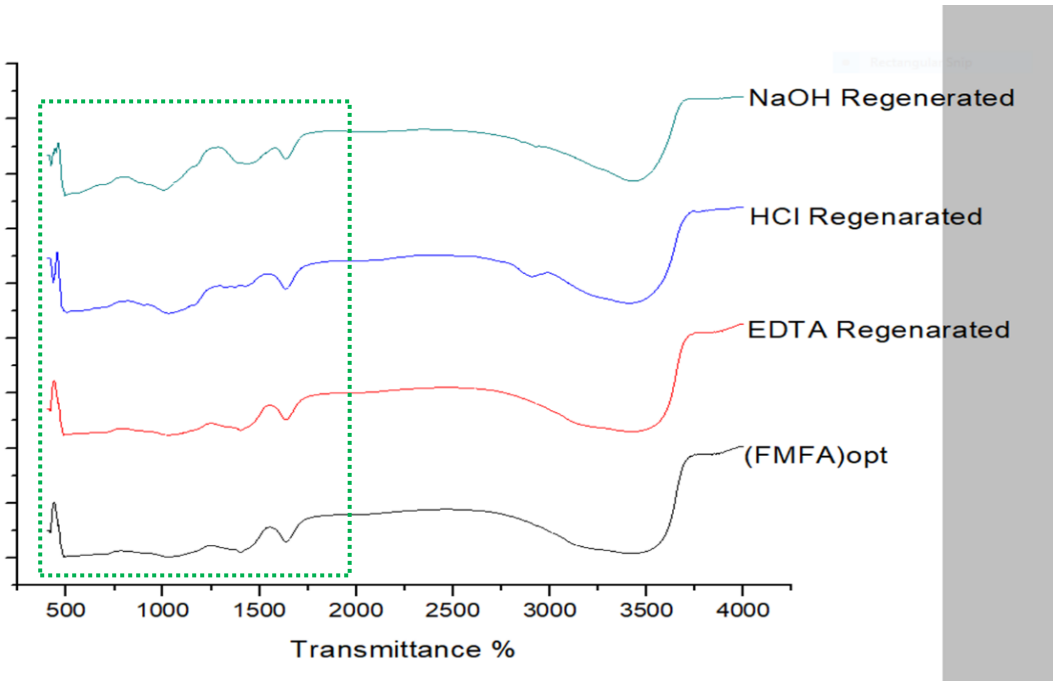

Figure 4.17 The FTIR spectra of regenerated $(FMFA)_{opt}$ were plotted after regeneration using the eluting agents of NaOH, HCL, and EDTA

After the regeneration, the surface functional groups of $(FMFA)_{opt}$ the peaks were decreased and increased, shifted and new peaks appeared. A drastic variation in the functional groups attributed for Fe and its related oxides lying on the region 500 cm^{-1} –

1500 cm^{-1} is observed. The strength of OH groups in regenerated materials have been decreased after the regeneration process compared to virgin $(FMFA)_{opt}$ may be due to the deterioration on the surface of the adsorbent.

4.9 Cost calculation for the synthesis of the defluoridation material

Cost For synthesis of MFA

Cost for Chemicals

Fly Ash (280g)	= Rs.0.00
HNO3 (10.00mL)	= Rs. 15.00
Distilled water (4L)	= Rs.40.00

Refluxing For the zeolite synthesis and Oven drying

Watt value of the refluxer	= 500W
Refluxing time	= 96Hrs
Total KWh for refluxer	= 24Kwh
Cost for refluxing	= Rs.240.00
Total cost to produce MFA	= Rs.295.00
Cost to produce 1.00g of MFA	= Rs.1.05

Cost For synthesis of FMFA

MFA (12g)	= Rs10.50
Deionized water	= Rs 22.00
FeCl3.6H20 (12g)	= Rs 0.97
Absolute Ethanol (2L)	= Rs 110.00
$NaBH_4$ (35.5g)	= Rs 60.45
Polyethylene glycol (1g)	= Rs.0.115

Watt Value for Oven = 800W

Drying time = 24Hrs

Total kWh =19.3KWh

Total cost for oven = Rs 193.00

Total cost for a synthetic cycle of FMFA = Rs.397.03

Approximately 25.00 g of FMFA is produced in a one synthetic cycle

Cost for 1g of FMFA = Rs.15.80.00

The volume of water required for 5 members family for three months= 900L

Assuming that the fluoride concentration in water is 2.00ppm and the whole material is exhausted within three months.

The weight of FMFA required for delfuoridation for three months =180.00g

The cost for material to refill after three months = 2844.00 Rs

The volume required for desorption of FMFA for 3 months = 6923.07 mL

The volume required for desorption of FMFA for 2 months = 4615.38 mL

The volume required for desorption of FMFA for 1 month = 2307.00 mL

The price of 50 mL 0.01 M NaOH solution = Rs. 0.63

The cost for desorption of FMFA after 3 months = Rs. 174.46

The cost for desorption of FMFA after 2 months = Rs. 116.03

The cost for desorption of FMFA after 1 month = Rs. 58.15

According to these calculations, the regeneration of materials increases the reusability of the materials and decrease the cost of materials compared to the refilling of adsorber by

new adsorbent. The exhausting point of the material was not studied using fixed bed column studies; therefore, the cost of actual material could be lower than the calculated value. A column studies followed by a breakthrough curve must be developed to know the exact exhausting time of the material.

5 CONCLUSIONS AND RECOMMENDATIONS

5.1 Conclusion

In this study, it was observed that the hardness and fluoride concentrations in potable groundwater must be lowered below 200.00 mg/L and 0.47 mg/L respectively to overcome the synergistic nephrotoxic effect of hardness and fluoride at their mutual presence. The hardness level is relatively very high in the CKDu prevalent areas and application of the synthetic Ion exchange resin (ECOA) was the ideal solution to remove excessive hardness other than utilizing bulks of low-cost adsorbents. Therefore, the development of an ion-exchange column was ideal and effective to remove excessive hardness in incoming water before utilizing water for the defluoridation.

The eluent coming from the ion-exchange column is rich in fluoride and, Ion oxide functionalized modified fly ash $(FMFA)_{opt}$ was a cost-effective and efficient defluoridation material.

The maximum fluoride removal was 10.00 mg for 1.00 g of $(FMFA)_{opt}$. The optimum defluoridation happened at pH 6.0. The material can be applied for defluoridation without changing the normal pH of potable groundwater. 40 minutes were taken for the defluoridation of 100.00 ml of the synthesized water as described in materials and methods to lower fluoride ion concentration from 2.10 mg/L to 0.33 mg/L. The fluoride adsorption mechanism fitted with the Langmuir adsorption isotherm model. Therefore, only a monolayer adsorption of fluoride on to the surface of the $(FMFA)_{opt}$ can be expected. The adsorption reaction followed pseudo-second-order kinetics therefore the adsorption mechanism is chemisorption.

The material refill cost for a family with 5 members was Rs 2,444.00 where the material regeneration cost was Rs.174.46. Therefore, the material is economical and affordable and efficient and can be recommended for commercialization to remove excessive fluoride in CKDu prevalent areas to overcome the hypothesis of nephrotoxicity of hardness and fluoride in their mutual presence.

5.2 Recommendations

Many studies are focussing on the nephrotoxicity of fluoride. Controversially, some studies report that there is no nephrotoxicity in the presence of fluoride ion alone in very high concentrations such as seven times higher than its MAL value given by WHO.

Therefore, a clear study to be undertaken to check whether there is a nephrotoxic effect of fluoride considering the water quality throughout the year in CKDu prevalent areas as the fluoride levels in water may change with climate. The nephrotoxicity of hardness and fluoride in their mutual presence was observed in this study and had been proven experimentally in previous studies. Therefore, water quality standards must be updated for the MAL of Fluoride in potable water in the presence of other ions especially hardness.

Further, the prevailing all possible factors for CKDu in CKDU prevalent areas to be strictly studied based on their biochemical mechanisms and their bioaccumulation in the kidney.

The defluoridation capacity of synthesized material is to be studied for different temperatures to check the ideal defluoridation temperature that gives the highest defluoridation. Further, a column study to be carried out to check the exact material required for a domestic filtration unit. Further, regeneration studies for different concentrations of NaOH have to be done to find the ideal NaOH concentration which can regenerate the material to give the highest defluoridation

Moreover, attention should be paid to synthesize more effective defluoridation materials such as Iron oxide modified mesoporous alumina to have a more positively charged surface with ah high surface area to increase the defluoridation A cost calculation has to be done to check the financial feasibility.

.

REFERENCES

Ayob, A. & Abdullah, A. Z. 2012 Characterisation of polymer-stabilized nano zero-valent iron particle by ultrasonic irradiation-assisted method. Journal of Polymer Materials29, pp.167–179.

Athuraliya, N.T., Abeysekera, T.D., Amerasinghe, P.H., Kumarasiri, R., Bandara, P., Karunaratne, U., Milton, A.H., and Jones, A.L., 2011. Uncertain etiologies of proteinuric-chronic kidney disease in rural Sri Lanka. Kidney International, 80(11), pp.1212-1221.

Athuraliya, T.N.C., Abeysekera, D.T.D.J., Amerasinghe, P.H., Kumarasiri, P.V.R., and Dissanayake, V., 2009. Prevalence of chronic kidney disease in two tertiary care hospitals: high proportion of cases with uncertain etiology. Ceylon Medical Journal, 54(1).

Auerbach, S.M., Carrado, K.A., and Dutta, P.K., 2003. Handbook of zeolite science and technology. CRC press.

Bhatnagar, A., Kumar, E., and Sillanpää, M., 2011. Fluoride removal from water by adsorption—a review. Chemical Engineering Journal, 171(3), pp.811-840

Barbier, O., Arreola-Mendoza, L. & Razo, D. L. M. 2010 Molecular mechanisms of fluoride toxicity. Chemico-BiologicalInteraction188(2), pp.319–333.

Bober, J., Kwiatkowska, E., Kedzierska, K., Olszewska, M., Stachowska, E., Ciechanowski, K. and Chlubek, D., 2006. Fluoride aggravation of oxidative stress in patients with chronic renal failure. Fluoride, 39(4), p.302.

Borke, J.L., and Whitford, G.M., 1999. Chronic fluoride ingestion decreases 45Ca uptake by rat kidney membranes. The Journal of nutrition, 129(6), pp.1209-1213.

Calafat, A.M., 2012. The US National Health and Nutrition Examination Survey and human exposure to environmental chemicals. International journal of hygiene and environmental health, 215(2), pp.99-101.

Carlson, C.H., Armstrong, W.D., and Singer, L., 1960. Distribution and excretion of radiofluoride in the human. Proceedings of the Society for Experimental Biology and Medicine, 104(2), pp.235-239.

Carton, R.J., 2006. Review of the 2006 United States National Research Council report: fluoride in drinking water. Fluoride, 39(3), pp.163-172.

Chandrajith, R., Nanayakkara, S., Itai, K., Aturaliya, T.N.C., Dissanayake, C.B., Abeysekera, T., Harada, K., Watanabe, T., and Koizumi, A., 2011. Chronic kidney diseases of uncertain etiology (CKDu) in Sri Lanka: geographic distribution and environmental implications. Environmental geochemistry and health, 33(3), pp.267278.

Chandrajith, R., Padmasiri, J.P., Dissanayake, C.B. and Prematilaka, K.M., 2012. Spatial distribution of fluoride in groundwater of Sri Lanka. Journal of the National Science Foundation of Sri Lanka, 40(4).

Chandrajith, R., Seneviratna, S., Wickramaarachchi, K., Attanayake, T., Aturaliya, T.N.C., and Dissanayake, C.B., 2010. Natural radionuclides and trace elements in rice field soils in relation to fertilizer application: study of a chronic kidney disease area in Sri Lanka. Environmental Earth Sciences, 60(1), pp.193-201.

Chouhan, S. and Flora, S.J.S., 2008. Effects of fluoride on the tissue oxidative stress and apoptosis in rats: biochemical assays supported by IR spectroscopy data. Toxicology, 254(1-2), pp.61-67.

Cittanova, M.L., Lelongt, B., Verpont, M.C., Geniteau-Legendre, M., Wahbe, F., Prie, D., Coriat, P. and Ronco, P.M., 1996. Fluoride ion toxicity in human kidney collecting duct cells. Anesthesiology: The Journal of the American Society of Anesthesiologists, 84(2), pp.428-435

Dharma-Wardana, M.W.C., 2018. Chronic kidney disease of unknown etiology and the effect of multiple-ion interactions. Environmental geochemistry and health, 40(2), pp.705-719.

Dharma-Wardana, M.W.C., Amarasiri, S.L., Dharmawardene, N. and Panabokke, C.R., 2015. Chronic kidney disease of unknown aetiology and groundwater ionicity: study based on Sri Lanka. Environmental geochemistry and health, 37(2), pp.221231.

Dissanayake, C.B. and Chandrajith, R., 2017. Groundwater fluoride as a geochemical marker in the etiology of chronic kidney disease of unknown origin in Sri Lanka. Ceylon Journal of Science, 46(2).

Freundlich, H.M.F., 1906. Over the adsorption in solution. J. Phys. Chem, 57(385471), pp.1100-1107.

Gifford, F.J., Gifford, R.M., Eddleston, M. and Dhaun, N., 2017. Endemic nephropathy around the world. Kidney international reports, 2(2), pp.282-292.

Ileperuma, O.A., Dharmagunawardhane, H.A. and Herath, K.P.R.P., 2009. Dissolution of aluminium from sub-standard utensils under high fluoride stress: a possible risk factor for chronic renal failure in the North-Central Province. Journal of the National Science Foundation of Sri Lanka, 37(3).

Ingallinella, A.M., Pacini, V.A., Fernández, R.G., Vidoni, R.M. and Sanguinetti, G., 2011. Simultaneous removal of arsenic and fluoride from groundwater by coagulation-adsorption with polyaluminum chloride. Journal of Environmental Science and Health, Part A, 46(11), pp.1288-1296.

Inkovaara, J., Heikinheimo, R., Jarvinen, K., Kasurinen, U., Hanhijarvi, H. and Iisalo, E., 1975. Prophylactic fluoride treatment and aged bones. Br Med J, 3(5975), pp.73-74.

Jayasekara, J.M., Dissanayake, D.M., Adhikari, S.B. and Bandara, P., 2013. Geographical distribution of chronic kidney disease of unknown origin in North Central Region of Sri Lanka. Ceylon Med J, 58(1), pp.6-10.

Jayasekara, K.B., Dissanayake, D.M., Sivakanesan, R., Ranasinghe, A., Karunarathna, R.H. and Kumara, G.W.G.P., 2015. Epidemiology of chronic kidney disease, with special emphasis on chronic kidney disease of uncertain etiology, in the north central region of Sri Lanka. Journal of epidemiology, 25(4), pp.275-280.

Jayasekara, K.B., Dissanayake, D.M., Sivakanesan, R., Ranasinghe, A., Karunarathna, R.H. and Kumara, G.W.G.P., 2015. Epidemiology of chronic kidney disease, with special emphasis on chronic kidney disease of uncertain etiology, in the north central region of Sri Lanka. Journal of epidemiology, 25(4), pp.275-280.

Jayasumana, C., Fonseka, S., Fernando, A., Jayalath, K., Amarasinghe, M., Siribaddana, S., Gunatilake, S. and Paranagama, P., 2015. Phosphate fertilizer is a main source of arsenic in areas affected with chronic kidney disease of unknown etiology in Sri Lanka. SpringerPlus, 4(1), p.90.

Jayasumana, C., Paranagama, P.A., Amarasinghe, M.D., Wijewardane, K.M.R.C., Dahanayake, K.S., Fonseka, S.I., Rajakaruna, K.D.L.M.P., Mahamithawa, A.M.P., Samarasinghe, U.D. and Senanayake, V.K., 2013. Possible link of chronic arsenic toxicity with chronic kidney disease of unknown etiology in Sri Lanka.

Jayatilake, N., Mendis, S., Maheepala, P. and Mehta, F.R., 2013. Chronic kidney disease of uncertain aetiology: prevalence and causative factors in a developing country. BMC nephrology, 14(1), p.180.

Jayawardana, D.T., Pitawala, H.M.T.G.A., and Ishiga, H., 2012. Geochemical assessment of soils in districts of fluoride-rich and fluoride-poor groundwater, northcentral Sri Lanka. Journal of Geochemical Exploration, 114, pp.118-125.

Jayawardana, D.T., Udagedara, D.T., Silva, A.A.M.P., Pitawala, H.M.T.G.A., Jayathilaka, W.K.P. and Adikaram, A.M.N.M., 2016. Mixing geochemistry of cold water around non-volcanic thermal springs in high-grade metamorphic terrain, Sri Lanka. Chemie der Erde-Geochemistry, 76(4), pp.555-565.

Jha, V., Garcia-Garcia, G., Iseki, K., Li, Z., Naicker, S., Plattner, B., Saran, R., Wang, A.Y.M. and Yang, C.W., 2013. Chronic kidney disease: global dimension and perspectives. The Lancet, 382(9888), pp.260-272.

Kakavandi, B., Jonidi, A., Rezaei, R., Nasseri, S., Ameri, A. and Esrafily, A., 2013. Synthesis and properties of Fe 3 O 4-activated carbon magnetic nanoparticles for removal of aniline from aqueous solution: equilibrium, kinetic and thermodynamic studies. Iranian journal of environmental health science & engineering, 10(1), p.19.

Karagas, M.R., Le, C.X., Morris, S.T.E.V.E.N., Blum, J.O.E.L., Lu, X.I.U.F.E.N., Spate, V.I.C.K.Y., Carey, M.A.R.K., Stannard, V.I.R.G.I.N.I.A., Klaue, B.J.O.E.R.N. and Tosteson, T.D., 2001. Markers of low-level arsenic exposure for evaluating human cancer risks in a US population. International journal of occupational medicine and environmental health, 14(2), pp.171-175.

Knez, S., Strazisar, J., Golob, J. and Horvat, A., 2001. Agglomeration of zeolite in the fluidized bed. Acta chimica slovenica, 48(4), pp.487-504.

Kosmulski, M., 2009. pH-dependent surface charging and points of zero charge. IV. Update and new approach. Journal of Colloid and Interface Science, 337(2), pp.439448.

Kovacheva, P., Arishtirova, K. and Vassilev, S., 2001. MgO/NaX zeolite as basic catalyst for oxidative methylation of toluene with methane. Applied Catalysis A: General, 210(1-2), pp.391-395.

Ku, Y. and Chiou, H.M., 2002. The adsorption of fluoride ion from aqueous solution by activated alumina. Water, air, and soil pollution, 133(1-4), pp.349-361.

Kumari, M.K.N., Pathmarajah, S., Dayawansa, N.D.K., and Nirmanee, K.G.S., 2016. Evaluation of groundwater quality for irrigation in Malwathu Oya cascade-I in the Anuradhapura District of Sri Lanka. Tropical Agricultural Research, 27(4), pp.310324.

Langmuir, I., 1938. Overturning and anchoring of monolayers. Science, 87(2266), pp.493-500.

Levine, K.E., Redmon, J.H., Elledge, M.F., Wanigasuriya, K.P., Smith, K., Munoz, B., Waduge, V.A., Periris-John, R.J., Sathiakumar, N., Harrington, J.M. and Womack, D.S., 2016. Quest to identify geochemical risk factors associated with chronic kidney disease of unknown etiology (CKDu) in an endemic region of Sri Lanka—a multimedia laboratory analysis of biological, food, and environmental samples. Environmental monitoring and assessment, 188(10), p.548.

Padilla, A. P., & Saitua, H. (2010). Performance of simultaneous arsenic, fluoride, and alkalinity (bicarbonate) rejection by pilot-scale nanofiltration. Desalination, 257(1-3), 16-21.

Paranagama, D., 2014. Chronic kidney disease of unknown origin in Sri Lanka and its relation to drinking water supplies: Doctoral dissertation

Petala, E., Dimos, K., Douvalis, A., Bakas, T., Tucek, J., Zboril, R. & Karakassides, M. A. 2013Nanoscale zero-valent ironsupported on mesoporous silica: characterization and reactivity for Cr(VI) removal from aqueous solution.Journal ofHazardous Materials261,pp. 295–306.

Pinon-Miramontes, M., Bautista-Margulis, R.G., Perez-Hernandez, A., 2003. Removalof arsenic and fluoride from drinking water with cake alum and a polymericanionic flocculent. Fluoride 36 (2), 122e128 (Research Report).

Ramesh, K. and Reddy, D.D., 2011. Zeolites and their potential uses in agriculture. In Advances in agronomy (Vol. 113, pp. 219-241). Academic Press.

Raul, P., Umlong, I. M. & Purkait, M. K. 2012Removal offluoride from water using iron oxide-hydroxide nanoparticles.Journalof Nanoscience and Nanotechnology12 (5), pp.3922–3930.

Rubasinghe, R., Gunatilake, S.K. and Chandrajith, R., 2015. Geochemical characteristics of groundwater in different climatic zones of Sri Lanka. Environmental earth sciences, 74(4), pp.3067-3076

Sudasinghe, M. I, 2016. “Water quality data of CKDu prevalent areas”, University of Moratuwa

Sudasinghe, M. et al., 2019. Defluoridation of calcium - rich groundwater using iron oxide nano particles. Water Practice and Technology, pp. 665-681.

Vithanage, M. and Bhattacharya, P., 2015. Fluoride in drinking water: health effects and remediation. In CO2 Sequestration, Biofuels and Depollution (pp. 105-151). Springer, Cham.

WHO (World Health Organisation). 2017Guidelines for Drinking Water Quality: 4th Edition Incorporating the 1st Addendum.Geneva, World Health Organization.

Zager, R. A. & Iwata, M. 1997 Inorganicfluoride divergent effects on human proximal tubular cell viability.American Journalof Pathology150(2), 735–743.